





Review

# Examining the Effects on a Fatigue Life of Preloaded Bolts in Flange Joints: An Overview

Ivan Okorn , Marko Nagode , Jernej Klemenc  and Simon Oman \* 

Faculty of Mechanical Engineering, University of Ljubljana, 1000 Ljubljana, Slovenia; ivan.okorn@fs.uni-lj.si (I.O.); marko.nagode@fs.uni-lj.si (M.N.); jernej.klemenc@fs.uni-lj.si (J.K.)

\* Correspondence: simon.oman@fs.uni-lj.si

**Abstract:** The amplitude of a bolt load in dynamically loaded bolted flange joints depends on several factors: the resilience of the bolt and the clamping parts, the magnitude of the working load, the point of action of the working load, the way the working load is transferred from the structure to the bolt, the preload, and the geometrical imperfections of the contact surfaces of the joint. These factors are analysed in many papers, and they are covered in the VDI 2230 guideline and in standards. Fatigue curves (S-N curves) of bolts are determined by tests in which an ideal axial load is usually applied to the bolts. The effects of the bolt strength class, the thread manufacturing process, the surface protection, and the cross-section size on the fatigue strength of bolts are precisely defined. The main problem in the evaluation of bolted joints is the calculation of the actual stress, which is compared with the fatigue curves. Despite extensive research, fatigue-related bolt failures still occur in practise. This article provides a systematic overview of the influences that affect the fatigue of bolts. The conclusions are based on the research results of many authors and on our own analytical, numerical, and experimental investigations. The effects are illustrated using two practical examples of flange bolting. The assessment of fatigue according to Eurocode 3 and the VDI 2230 guideline is discussed in more detail.

**Keywords:** flange joint; preload; working load; bolt fatigue life; geometrical flange imperfections



**Citation:** Okorn, I.; Nagode, M.; Klemenc, J.; Oman, S. Examining the Effects on a Fatigue Life of Preloaded Bolts in Flange Joints: An Overview. *Metals* **2024**, *14*, 883. <https://doi.org/10.3390/met14080883>

Academic Editor: Xudong Qian

Received: 14 June 2024

Revised: 22 July 2024

Accepted: 25 July 2024

Published: 31 July 2024



**Copyright:** © 2024 by the authors. Licensee MDPI, Basel, Switzerland. This article is an open access article distributed under the terms and conditions of the Creative Commons Attribution (CC BY) license (<https://creativecommons.org/licenses/by/4.0/>).

## 1. Introduction

Bolted joints are the most common type of detachable joints in parts and structures. In this paper, we will limit our scope to bolted flange joints. Two major specific application areas for bolted flange joints should be highlighted: piping and pressure vessels [1,2], and steel structures [3–9]. Examples of steel structures are wind turbine towers, chimneys, cableway columns, steel bridges, and truss structures. A bolted joint consists of several bolts and two flanges. The flanges are always circular in pipelines, whereas in the case of load-bearing structures, they are either circular or rectangular. A gasket is inserted between the flanges in pipelines and pressure vessels to prevent the medium from flowing out of the pipeline or pressure vessel. To ensure the sealing effect, the gasket must be uniformly compressed with the specified force even when the joint is subjected to a working load due to the pressure in the pipeline. Therefore, bolts must be preloaded during installation. In steel structures, high-strength bolts of class 10.9 are generally used, and they are preloaded to approximately 70% of the bolt yield strength. The main objective of preloading is to reduce the fluctuating load of the bolts under the applied dynamic working load.

The basic theory of preloaded bolted joints is covered in the general literature on machine elements, steel structures, and pressure vessels [10–12]. Understanding the force–displacement diagram is crucial for understanding the effects on the dynamic loading of bolts and, consequently, on bolt fatigue. This paper will first analyse the factors that affect the shape of the diagram in detail, in particular the additional load on the bolt. Methods for determining the resilience of the bolt and the clamping parts will be given. The magnitude

of the additional bolt load depends on how and where the working load is applied to the joint and how it is transferred to the bolts. In practise, the working load is generally not applied directly under the bolt head or in the bolt axis. Examples will be given to explain how the location of the load introduction affects the dynamic load and the stress in a bolt.

The size and location of the bolt's working load can be easily determined in very few practical applications. In the case of flanged pipe joints and pressure vessel covers, the working load is calculated as the product of the pressure and the surface to which the pressure is applied. The load on the individual bolts is calculated by dividing the total load by the number of bolts. In the case of pipelines, the calculation is simple if the weight of the pipeline (which exerts an additional bending moment on the joint) is neglected. Even for a simple cantilever beam loaded with a bending moment, there is no exact analytical method to calculate the working load on a bolt. In one of our previous studies [13], the loads in individual bolts fixing a rectangular flange were determined numerically and experimentally. An analytical method has been developed to determine the working load in each bolt. The results obtained with this new method were compared with those of other approaches. Determining the working load per bolt in complex load-bearing structures is much more difficult. The current application of flange joints are connections of tower segments of wind turbines [14]. In the case of fixed towers, the joint is loaded by the dead weight of the tower and the bending moment resulting from the forces acting on the wind turbine. As the direction and magnitude of the forces change over time, so does the working load in each bolt. The load situation is much more complex in floating wind farms [15] because of the additional effect of waves. This paper presents approaches to determine the working load in the bolts based on the external dynamic loads on the structure.

In a preloaded bolted joint, an axial force is applied to the bolt during assembly to compress the parts between the bolt head and the nut. The most common method of bolt assembly is using a torque wrench or other suitable tightening tool to tighten the bolt to the specified torque. The analytical relationship between the axial force in the bolt and the tightening torque involves a coefficient of friction, which has a very large scatter. The actual preload may, therefore, deviate considerably from the theoretically assumed preload. Another, more complex assembly method involves applying a tensile force to the bolt by using a special device that stretches the bolt before tightening the nut. The nut is then tightened to its final position without any additional torque being applied. Therefore, only normal stress due to the axial force appears in the bolt during tightening. The actual preload in a particular bolt is influenced not only by the way the bolt is tightened but also by the sequence in which the bolts are tightened and the number of tightening steps until the final preload value is reached. Details of bolt tightening, particularly the effect of bolt preload on bolt fatigue, are presented and analysed in Section 5.

It is not possible to manufacture the elements of a bolted joint with a perfectly ideal geometry. The contact surfaces of the flanges are not flat, so a gap between the flanges occurs before assembly. In this article, we will focus on the effects of geometric imperfections on the fatigue of bolts in round flanges. With small flange diameters, a gap may occur either on the pipe side or on the flange side. Especially with large flange diameters, which are designed with many bolts, a parallel gap often occurs around the circumference of the flange. Large flanges are welded to the pipe, while the contact surfaces are not machined after welding. Studies show that the actual fluctuating load on the bolts which are located in the area where the gap exists is significantly higher than the theoretical load [16]. The influence of flange imperfections on fatigue is dealt with in Section 6.

Only when the actual stress in the bolt cross-section is known, which is significantly influenced by the factors mentioned above, can the fatigue life of the bolt be estimated. The fatigue load capacity of bolts is determined by dynamic tests, which are used to generate S-N curves for different probabilities of critical failure. In the evaluation according to VDI 2230 [17], the amplitude stress in the bolt is compared with the allowable amplitude stress. The Eurocode 3 standard [18] is often used to evaluate bolts in steel structures. This standard defines the change of nominal stress in the bolt  $\Delta\sigma_c$  at which fatigue failure of the

bolt occurs after a certain number of loading cycles. The relationship between the change in nominal stress (also known as the stress range) and the number of load cycles is given by the S-N curve. A design detail is defined by the stress range  $\Delta\sigma_c$  at which the bolt can withstand  $2 \times 10^6$  load cycles. The effects on the shape of the S-N curve and the fatigue verification method are discussed in the last section.

The above-mentioned effects on fatigue, which are discussed in detail in the individual sections, are shown in Figure 1.

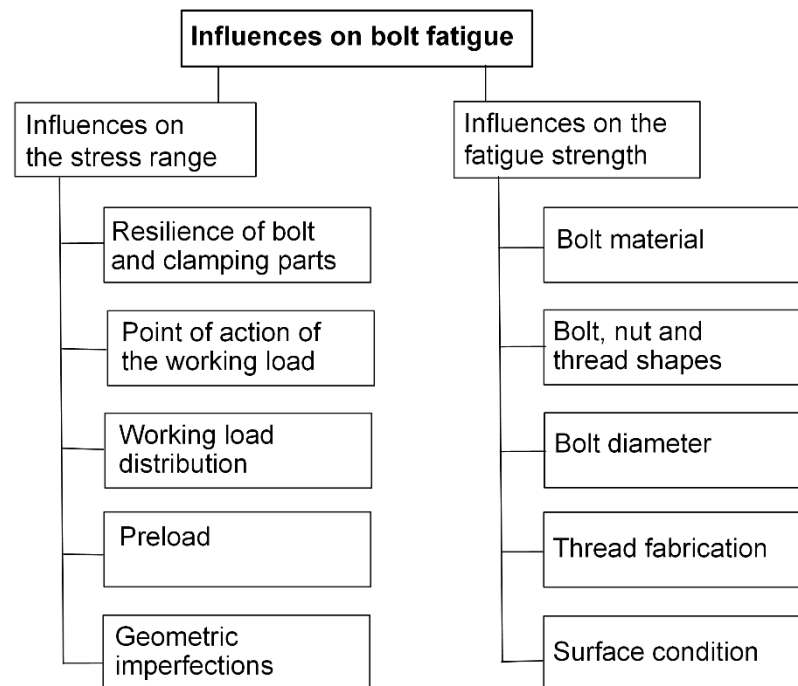


**Figure 1.** Effects on fatigue of preloaded bolts.

## 2. Influence of Resilience of Bolt and Clamping Parts on the Fluctuating Load of the Bolt

The force–displacement diagram displays the theoretical conditions of a preloaded bolt (Figure 2). The symbols and indices for forces and strains are taken from the VDI 2230 guideline [17]. A distinction must be made between the preload and the operating conditions. The dashed line shows the diagram at preload. When the bolt is loaded with a preload  $F_V$ , it is stretched by  $f_S$ , and the clamping parts are contracted by  $f_P$ . The elongation depends on the stiffness of the bolt  $k_S$  and the stiffness of the clamping parts  $k_P$ . During operation, when the working load  $F_A$  is applied to the bolted joint, the load in the bolt is increased, and the load between the clamping parts (sealing force  $F_K$ ) is decreased. In a special case, when the working load is applied at the same point as the preload, the stiffness of the joint during operation is the same as that of the preload. In practise, only part of the clamping parts are relieved, and part of the clamping parts continue to be compressed, contributing to a flatter  $k_{S^*}$  and a steeper  $k_{P^*}$  characteristic. In VDI 2230, this effect is taken into account by the load introduction factor. The variation in the working load during operation leads to a variation in the additional bolt load, which is critical for the bolt fatigue. It can be seen from the diagram that the amplitude of the dynamic load on the bolt is reduced if the bolt is less stiff (i.e., more elastic) and the clamping parts are stiffer. Detail A, which shows a variation in the additional load in the bolt, is crucial for analysing the bolt fatigue. This part of the diagram is linear only if the working force is applied along the axis of the bolt, which is very rare in practical applications. In flange joints, the working load is applied eccentrically, and the additional load on the bolt increases progressively due to the additional bending load (on bolt and flange). When dealing with the fatigue of bolts, an

increase in the additional bolt load as a function of the working load is usually specified, as shown in Figure 3.

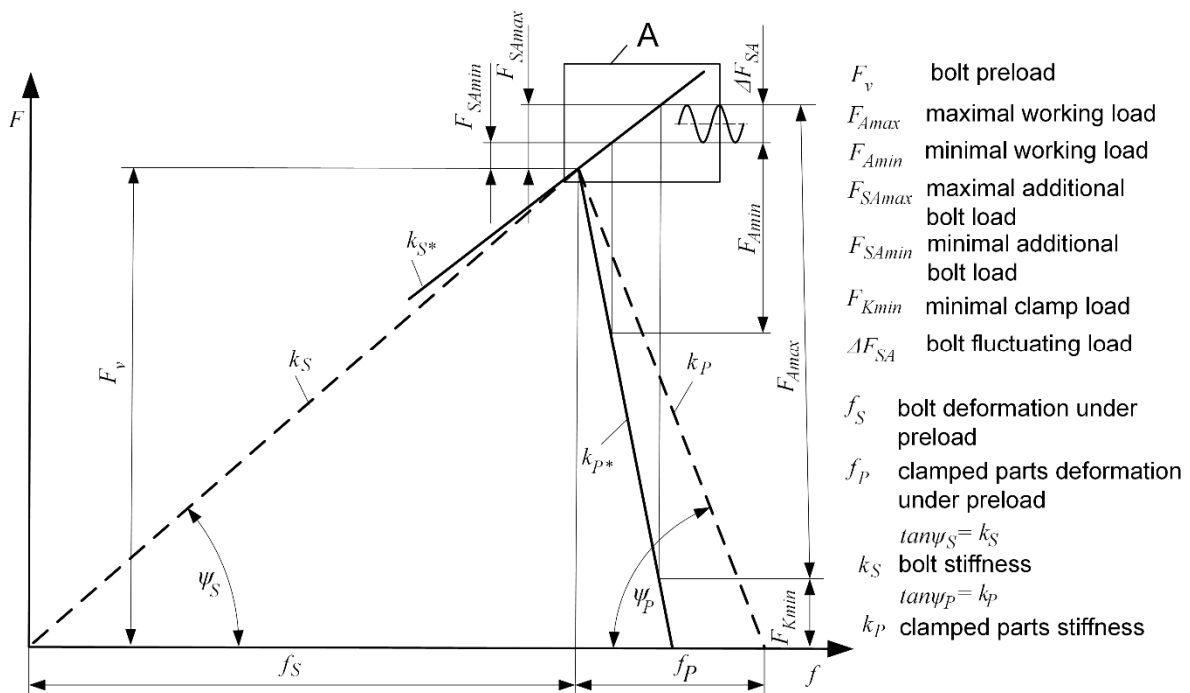


Figure 2. Load–deformation diagram.

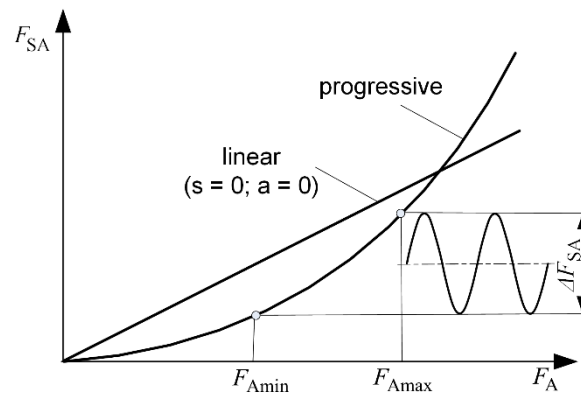


Figure 3. Additional load on the bolt as a function of the working load.

The theoretical stiffness of a standard bolt can be calculated analytically with relative ease. It depends on the cross-section of the bolt  $A$ , the length of the bolt  $l$  (only the part that is loaded), and the modulus of elasticity  $E$ . Bolts have several different cross-sections  $A_i$  with different stiffnesses  $k_{si}$  along their length. The reciprocal value of the stiffness is resilience. A bolt is considered to be a series of springs connected in series. The resilience of a bolt is the sum of the resilience values of the individual segments of the bolt.

$$\delta_S = \frac{1}{k_S} = \sum_{i=1}^n \frac{1}{k_{Si}} = \sum_{i=1}^n \frac{l_i}{A_i \cdot E_i} \tag{1}$$

In addition to the resilience of individual parts of the shank  $\delta_1, \delta_2 \dots$ , VDI 2230 also takes into account the resilience of the head part of the bolt  $\delta_K$ , the resilience of the part of the bolt that is threaded into the nut  $\delta_G$ , and the resilience of the nut  $\delta_M$ . The standard design of the nut is not optimal in terms of bolt fatigue. The load is distributed unevenly

on the thread and the notch effect coefficient, which is decisive for the fatigue of the bolt, is high. Using more elastic nuts [19] can reduce the notch effect on the bolt and increase the total resilience. Both effects have a positive impact on the fatigue life of bolts.

$$\begin{aligned}\delta_S &= \delta_K + \delta_1 + \delta_2 + \dots + \delta_G + \delta_M \\ \delta_S &= \frac{1}{E_S} \cdot \left( \frac{0.4 \cdot d}{A_N} + \frac{l_1}{A_1} + \frac{l_2}{A_2} + \dots + \frac{0.5 \cdot d}{A_3} + \frac{0.4 \cdot d}{A_N} \right)\end{aligned}\quad (2)$$

The resilience of clamping parts is the sum of the resilience of individual segments that are subjected to a compressive load. In the case of washers, the shape of a compressively loaded section is a circular ring with a known outer and inner diameter. Therefore, a washer's resilience can be calculated analytically and accurately. The calculation of the resilience of the flanges is a more difficult problem. Various analytical equations have been derived from numerical analyses, but they do not give exactly the same results. A comparison of different approaches in a practical case is given in [20–22]. Several authors [23–26] described a compression zone with hollow truncated cones (Figure 4). In practise, the Equations (3) and (4), recommended by VDI 2230 [17], are mostly used today. Geometric values for calculating the resilience of coupling parts are indicated in Figure 4. The wrench size is used as the contact diameter  $d_w$  for hex-head cap bolts, while the head diameter is used as the contact diameter  $d_w$  for cylindrical-head bolts. The pressure cone angle  $\varphi$  is approximately  $30^\circ$  and varies slightly depending on the joint geometry. The shape of the deformed zone in a nut connection is not the same as in a bolt that is threaded into a structure. This difference is taken into account by a parameter  $w$ :  $w = 1$  for the nut connection (example in Figure 4) and  $w = 2$  for the bolt threaded into the structure.

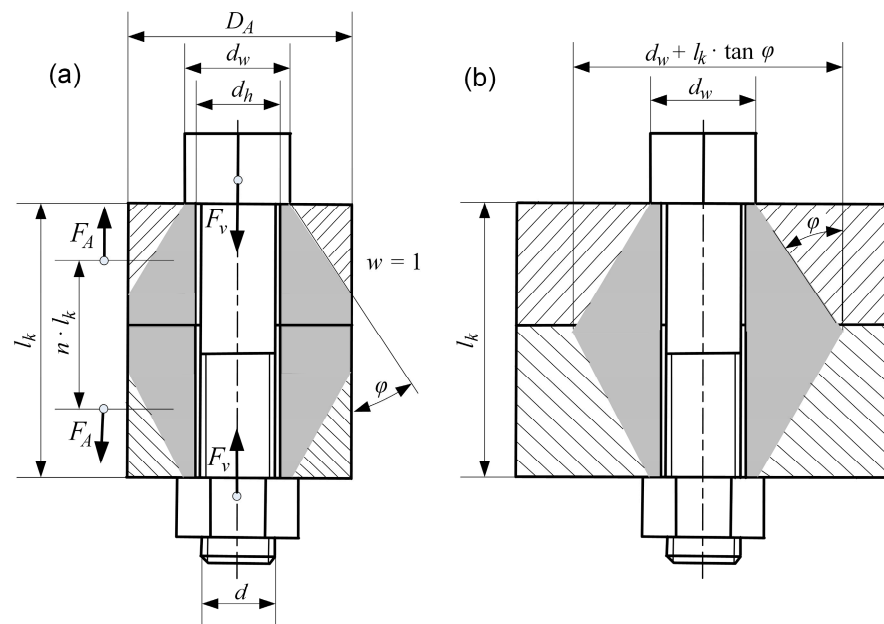


**Figure 4.** Pressure zone represented by pressure cones: (a) partially developed pressure cone and (b) fully developed pressure cone.

For  $d_w < D_A < (d_w + w \cdot l_k \cdot \tan \varphi)$  on Figure 4a:

$$\delta_P = \frac{2}{w \cdot d_h \cdot \tan \varphi} \ln \left[ \frac{(d_w + d_h) \cdot (D_A - d_h)}{(d_w - d_h) \cdot (D_A + d_h)} \right] + \frac{4}{D_A^2 - d_h^2} \left[ l_k - \frac{D_A - d_w}{w \cdot \tan \varphi} \right] \quad (3)$$

For  $D_A \geq (d_w + w \cdot l_K \cdot \tan\varphi)$  on Figure 4b:

$$\delta_P = \frac{2 \cdot \ln \left[ \frac{(d_w + d_h) \cdot (d_w + w \cdot l_K \cdot \tan\varphi - d_h)}{(d_w - d_h) \cdot (d_w + w \cdot l_K \cdot \tan\varphi + d_h)} \right]}{w \cdot E_P \cdot \pi \cdot d_h \cdot \tan\varphi} \tag{4}$$

Equations (3) and (4) apply only to flanges. If there is a washer under the bolt head or the nut, the washer resilience must be added to the calculation of the joint’s total resilience  $\delta_P$ .

An analytical calculation of the resilience of the bolted flange joint in Figure 5 is given in [27]. The dimensions of the DN40 flanges with four bolts around the circumference correspond to the EN1092 standard [28] for pipe flange joints. There is an insert with a nominal thickness of 4.4 mm between the flanges. The resilience of the elongated bolt is  $\delta_{SA} = 3.06 \times 10^{-6}$  mm/N, and the resilience of the short bolt is  $\delta_{SB} = 1.53 \times 10^{-6}$  mm/N. If the insert is made of steel, the resilience of the clamping parts is  $\delta_{PA} = 1.07 \times 10^{-6}$  mm/N and  $\delta_{PB} = 3.2 \times 10^{-7}$  mm/N.

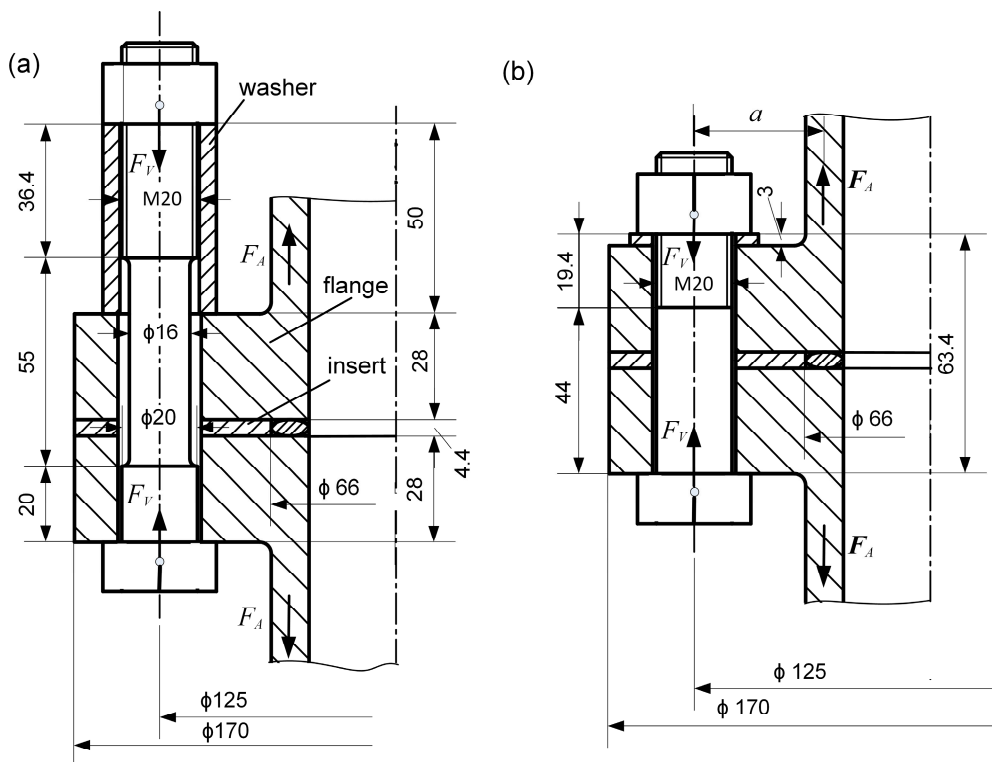


Figure 5. Examples of bolted flange joints: (a) example with elongated bolt and (b) example with short bolt; Adapted from ref. [27].

The relationship between the additional load on the bolt and the working load is described by a load factor.

$$\varnothing_e = \frac{F_{SA}}{F_A} = \frac{\delta_P}{\delta_S + \delta_P} \tag{5}$$

The equation shows that the additional load on the bolt is lower if the bolt is more elastic and clamping parts are more stiff. Long (elastic) bolts are, therefore, used in bolted joints that are dynamically loaded. In internal combustion engines, such bolts are used in the connection between the cylinder head and cylinder block as well as in the piston rod connection. The fatigue of elastic bolts is discussed by Griza et al. [29–31] in their studies.

The stiffness of bolted joints is significantly influenced by the surface morphology. Real surfaces have a roughness with unevenness that deforms both elastically and plastically under load. It is generally known that the elasticity of these surface irregularities reduces

the overall stiffness of the bolted joint. Chang et al. [32] study the contact stiffness of bolted joints in precision machine tools, derive algorithms for stiffness calculation, and analyse the effects of contact stiffness on vibration and machine tool precision. Similarly, Yiang et al. [33] investigate the effect of contact surface stiffness on the overall stiffness of bolted joints by using the energy method to determine the stiffness of individual elements. Their study also considers the influence of the friction coefficient on the stiffness. For a selected bolted joint geometry, the stiffness values are calculated using the proposed method and compared with traditional methods such as VDI 2230 and the Shigley method. A quantitative example of influence of resilience of bolt and clamping parts on bolt fatigue is shown in Appendix A.1 (see Figure A1 and Table A1).

### 3. Effect of the Point of Action of the Working Load on the Fluctuating Load on the Bolt

In practical applications, the working load usually does not act in the bolt axis and does not act directly under the bolt head. The additional load on the bolt is also influenced by the point of action of the working load, which is taken into account by the VDI 2230 guideline [17] with a working load point of action coefficient  $n$ , which defines how much the clamping parts are relieved when the working load is applied. The smaller the proportion of relieved clamping parts, the smaller the coefficient. For the joints in Figure 5,  $n$  is significantly smaller for design (a) as the entire washer is not relieved but is compressed further when the working load is applied. If the point of action of the working load is taken into account, Equation (5) is converted into the following:

$$\varnothing_{en} = \frac{F_{SA}}{F_A} = n \cdot \frac{\delta_P}{\delta_S + \delta_P} \quad (6)$$

The equation applies to a centric preload if the compression zone is symmetrical to the bolt axis, and the working load is applied in the bolt axis (centric loading). Cornwell [34] has numerically determined the force relationships for centric loading for various clamping part materials and geometries. He derived an equation for calculating the force relationships on the basis of numerical analyses. Concentrically loaded bolted joints were also investigated numerically and experimentally by Cardoso et al. [20]. His results agree very well with those obtained using the VDI 2230 guideline. In most practical applications, the working load is applied eccentrically at a certain distance from the bolt axis. The bolt is additionally subjected to bending and the surface pressure on the clamping surfaces is not evenly distributed. The VDI 2230 guideline [17] also defines a general analytical calculation method for eccentric loading and eccentric preload. Modified resiliencies  $\delta_P^{**}$  and  $\delta_P^*$  are used in Equation (7) to take into account both the eccentricity of the working load  $\delta_P^{**}$  and the eccentricity of the preload  $\delta_P^*$ . The values for the cases in Figure 5 are calculated in [27].

$$\varnothing_{en}^* = \frac{F_{SA}}{F_A} = n \cdot \frac{\delta_P^{**}}{\delta_S + \delta_P^*} \quad (7)$$

The linear theoretical relationship is valid as long as a compressive load occurs on the entire contact surface of the flanges (Figure 6a). Due to the eccentricity of the working load, the pressure on the side from which the working load is applied decreases as the working load increases. When a gap forms between the flanges (Figure 6b), the relationship between the working load and the additional bolt load is no longer linear. From the point when only the edge point is in contact (Figure 6c), the additional force can theoretically be determined from the equilibrium equation for the lever. The axis of the bolt is denoted by S-S, the axis of symmetry of the pressure zone by O-O, the eccentricity of the bolt axis with respect to the axis of the pressure zone by  $s$ , and the eccentricity of the working load with respect to the axis of the pressure zone by  $a$ . The design of the joint should aim to minimise the value of  $a$  and maximise the value of  $v$ . The characteristic of the joint also depends on the flange thickness  $h$ .

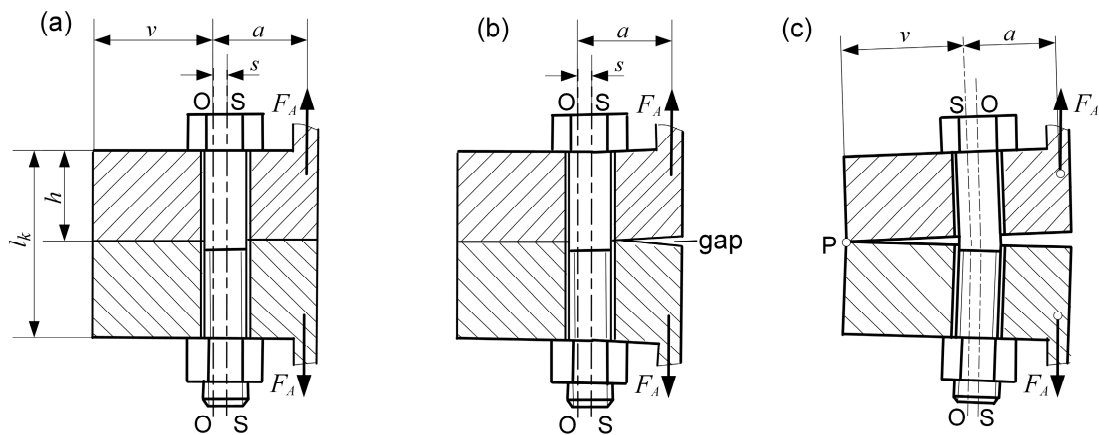


**Figure 6.** Bolt load conditions under eccentric working load: (a) working load too small for a gap to appear, (b) working load big enough for a gap to appear and (c) working load so big that only one point remains in contact.

Figure 7 shows the relationship between the additional load in the bolt and the working load for the three loading conditions mentioned above. The states (a) and (c) are connected by an arc in the VDI 2230 guideline. Equations for the analytical calculation of the limit points 1 and 2 and the radius of the arc are derived in the literature [19]. Schmidt and Neuper [35] have simplified the theoretical dependence between the additional bolt load and the working load by three lines, and Petersen [36] by two lines.

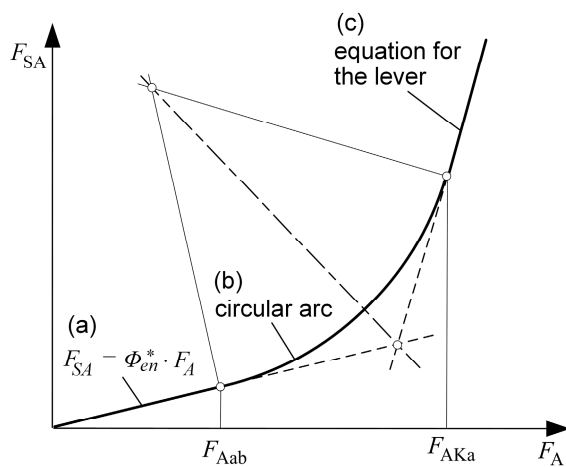


**Figure 7.** Graphical representation of the relationship between the additional load in the bolt and the working load: regions (a), (b) and (c) correspond with states shown in Figure 6 under the same letter; Adapted from ref. [17].

Since not all parameters required for an analytical study can be determined precisely, the finite element method is increasingly being used to determine the fluctuating load on a bolt. The studies of many authors [37–39] show a progressive relationship between the additional load on the bolt and the working load. In most studies, the results of the numerical analyses were verified by measuring the forces on the bolts. The results of our study [27] for the flange joints shown in Figure 5 are shown in Figure 8. The additional load on the bolt is negligible at low working loads, regardless of the design. As the working load increases, the additional load on the bolt increases progressively. The symbols in Figure 8 indicate HW = high washer, LW = low washer, and MB = modified bolt. The modified bolt differs from the standard bolt since its diameter is reduced to 16 mm. It can be seen from Figure 8 that the additional load on the bolt can be significantly reduced by using a high washer.



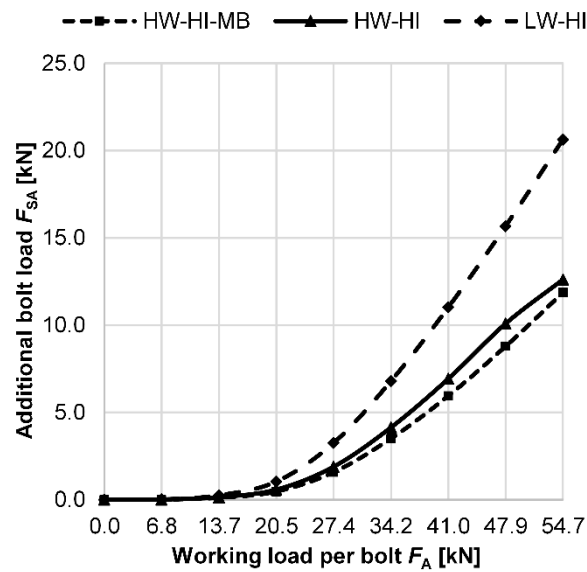


Figure 8. Additional bolt load, depending on the working load; Adapted from ref. [27].

Accurate calculation of the stress–strain state in flange joints is extremely complicated, regardless of whether the load is applied symmetrically or asymmetrically on the joint. Due to the geometry of the flange, the pressure cones cannot develop evenly in all directions in many practical cases. This leads to an asymmetrical compression load zone, which causes bending stresses in the bolt already at preload. As expected, the percentage of the bending load compared to the axial load increases with increasing working load (Figure 9). The stress distribution over the bolt cross-section for the two cases presented in [27] is shown in Figure 10. A more favourable stress distribution over the bolt cross-section is obtained by using a high washer. A quantitative example which clearly shows the effect of the point of action of the working load on bolt fatigue is shown in Appendix A.2 (see Figure A2 and Table A2).

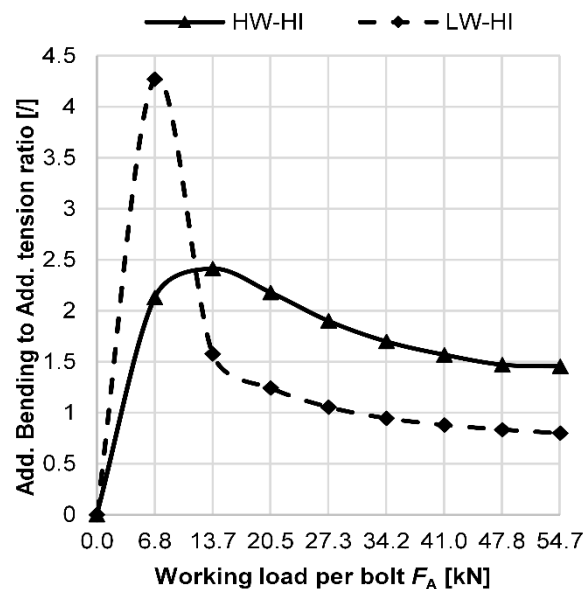
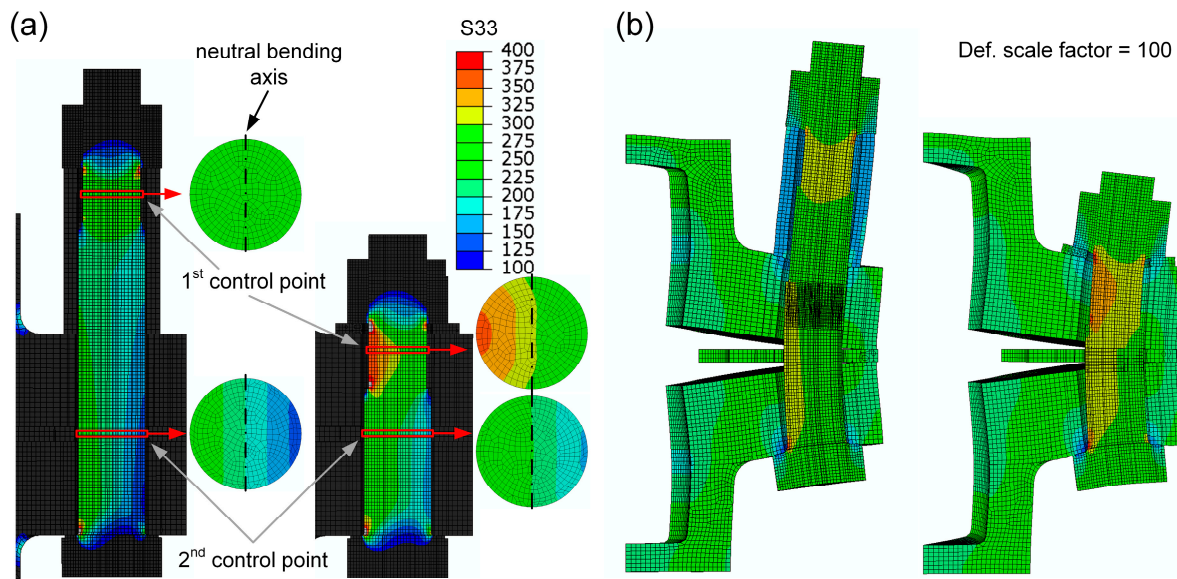


Figure 9. Relationship between bending and axial load on a bolt; Reprinted from ref. [27].



**Figure 10.** Stress distribution across the bolt cross-section: (a) result with realistic deformations and (b) result using deformation scale factor of 100; Adapted from ref. [27].

#### 4. Calculation of the Working Load Per Bolt Based on the Realistic Load on the Structure

Flanges are normally connected using several bolts. Based on the external load, the working load acting on each bolt must be calculated first. There are several methods for calculating the working load on bolts for the connection of end-plates and flanges. Oman and Nagode discuss in their study [13] the calculation of forces in bolts for fastening an end-plate cantilever beam. The connection in Figure 11 is loaded by a bending moment and a transverse force. By preloading the bolts, the normal force is applied to the contact surfaces, creating friction that prevents the flange from slipping. The required clamping force per bolt is calculated under the condition that the frictional force must be greater than the transverse force. After the bolts have been installed and properly preloaded, the clamping force is equal to the preload force on the bolt. In the case of a loaded connection, an additional tensile load (working load) is applied to some bolts, which causes a reduction in the clamping force. Thus, the individual bolts contribute in different proportions to the total residual clamping force on the contact surface of the end-plate. In the study of Oman and Nagode, an analytical method was developed to calculate the working loads in the bolts. Based on the normal stress occurring in the beam, the magnitude and position of the total normal force on the connection is determined. The calculation is performed separately for the tension and compression regions (see Figure 11). The load on the individual bolts is then calculated using the equilibrium equation.

$$F_{A1} = \frac{1}{2} \cdot \left( F_N \cdot \frac{a}{a+b} \right) \quad (8)$$

The working loads in eight M16 bolts were determined for two different beam shapes (IPE 120 beam and T-beam) and two end-plate thicknesses (12 mm and 20 mm). Finite element analyses were performed for all four connection combinations. The results were verified by an experiment using the connection shown in Figure 11. Figure 12 shows the results of the analytical calculation and the FE analysis for the I-beam and two values of the end-plate thickness. The following values were used in the calculation: beam load  $F = 10$  kN applied at a distance of  $r = 400$  mm from the end-plate connection and a preload on each bolt  $F_v = 32$  kN. The results of the new analytical method are in agreement with the results of the FE analysis. The gained results were also compared with those calculated using other analytical methods. The analysis shows that the most heavily loaded bolts are in the second row and not in the first row as calculated with the other four methods.

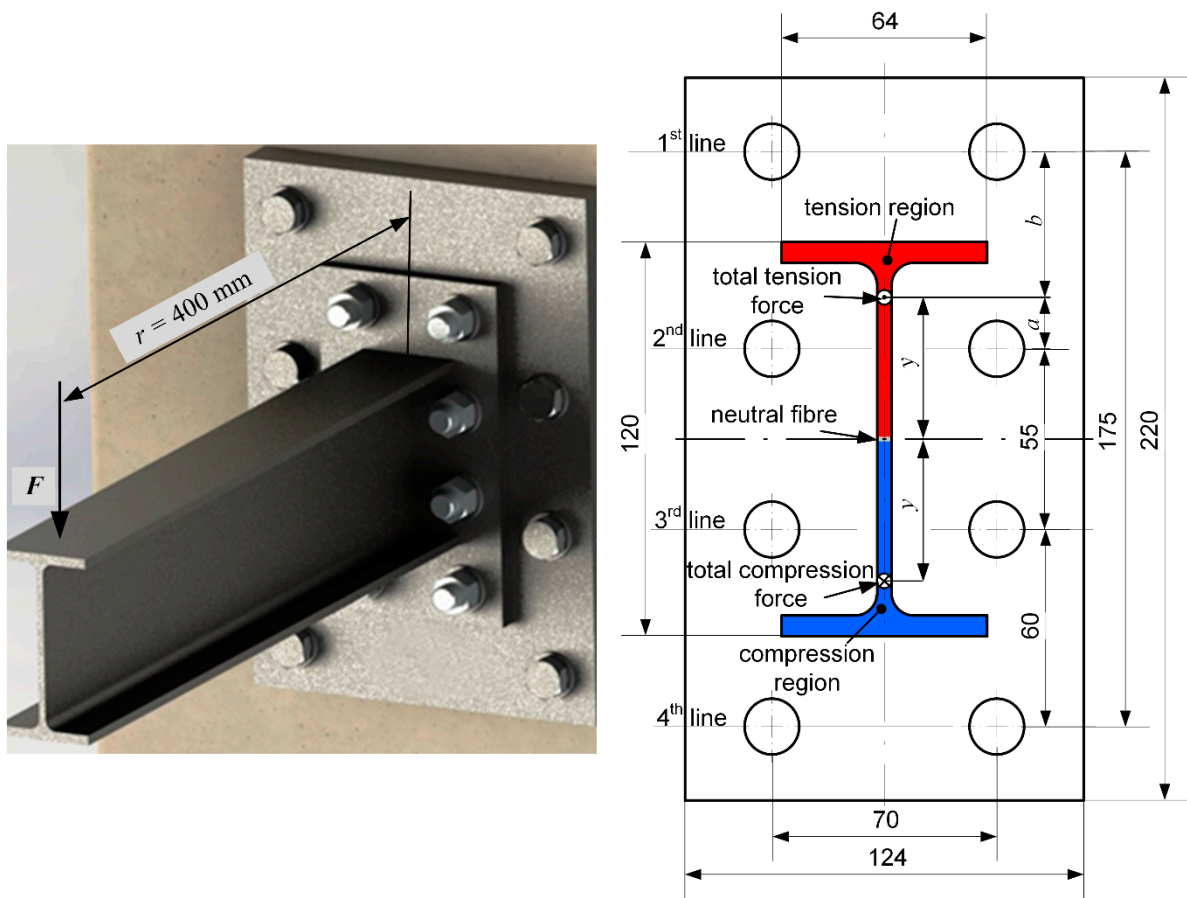


Figure 11. Layout of the bolts for fixing the end-plate connection; Adapted from ref. [13].

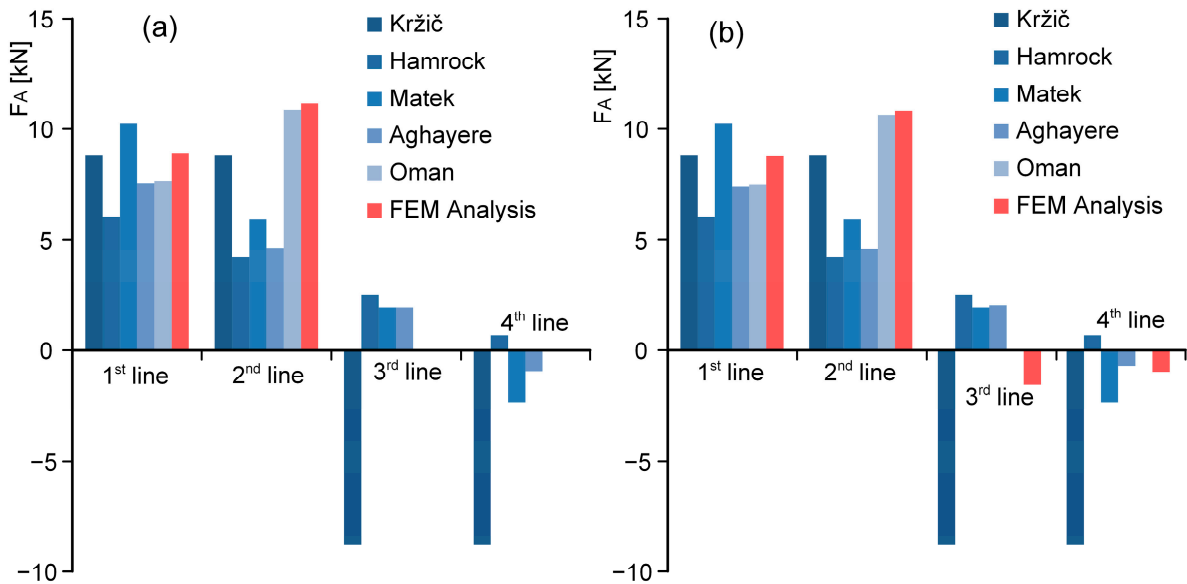
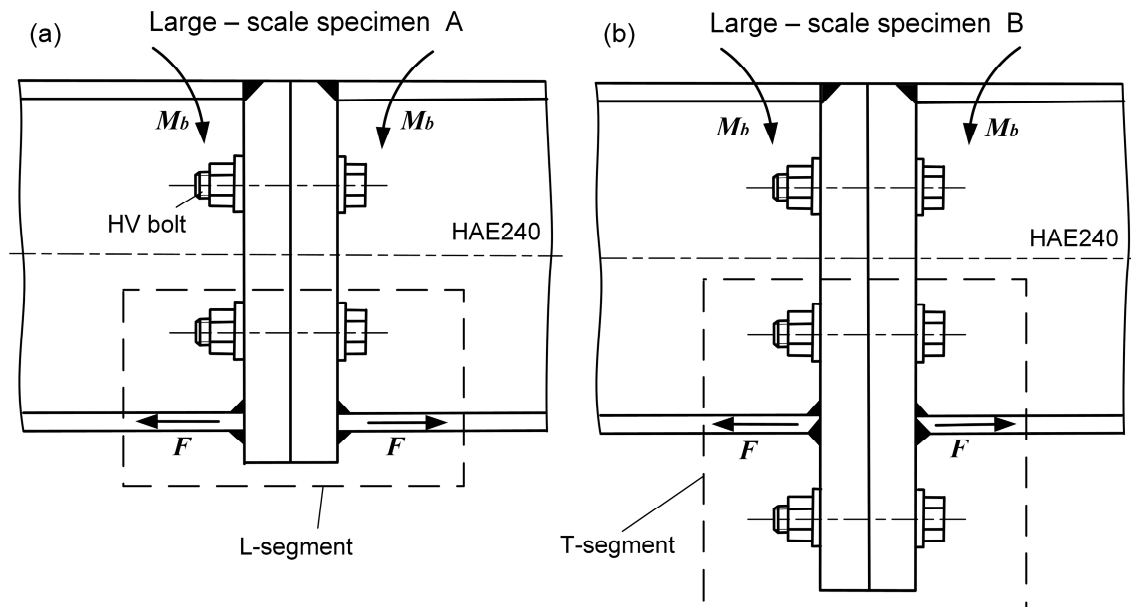


Figure 12. Working loads on bolts calculated by different methods: (a) flange thickness of 12 mm and (b) flange thickness of 20 mm; Adapted from ref. [13].

Some other researchers have also analysed end-plate connections using the finite element method and have come to similar conclusions [40–45]. One of the most recent studies was carried out by Bartsch et al. [46,47]. They investigated a HAE 240 beam connected in the middle by two 30 mm-thick end-plates with preloaded bolts. The beam

was then subjected to a four-point bending test to load the bolts. The A-type end-plates were connected with four bolts, while the B-type end-plates were connected with six bolts (see Figure 13). The authors assume that the entire tensile force is applied to the joint at the point where the lower beam flange is connected to the end-plate (shown with arrows in Figure 13 and labelled  $F$ ), and that in the case of the B-type end-plate, the two lower bolt rows carry the same working load.



**Figure 13.** Bolt layout in end-plate connections: (a) A-type end-plate and (b) B-type end-plate; Reprinted with permission from ref. [47]. Copyright (2024), with permission from Elsevier.

The investigation comprised six four-point bending fatigue tests on the entire beam with different end-plate connections (large-scale specimens) and, additionally, six tensile fatigue tests on L-segments (see the area marked with dashed lines in Figure 13a), and 12 tension fatigue tests on T-segments (see the area marked with dashed lines in Figure 13b) which were designated as small-scale specimens. The tests were used to determine the fatigue strength of the bolts and welds. The results were presented as S-N curves. For the A-type end-plate joint, the bolts were the more critical elements, while weld failure was more likely to occur in the B-type end-plate joint.

For circular flanges, the working load per bolt is determined based on the normal stress in the pipe. The circumference of the pipe is divided into several segments, each of which is connected by a bolt. The working load per bolt is the product of the stress in the segment and the area of the segment. This model is used by researchers working on flange joints in wind turbine towers [37–39]—it is called the segment model. In wind turbines, the bolts are located on the inside of the tube (L-segment) and are not visible from the outside. Large-diameter joints can also be constructed with flanges bolted on both sides of the tube. In this case, there are two bolts in each segment (T-segment) so that the working load on each bolt is half the load on the segment. A more accurate, but also more complex, calculation of bolt loads in round flanges is described in [48,49]. An example which shows the precision of different established methods to define the working force distribution in case of I-Beam cantilever beam is shown in Appendix A.3 (see Figure A3 and Table A3).

## 5. Effect of Preload on the Clamping Force and Bolt Fatigue

When evaluating flange joints, the working load  $F_A$  and the required clamping force  $F_K$ , which provides the surface pressure on the contact surfaces, are usually known. For pipe joints with gaskets, the surface pressure on the gasket is specified to ensure that the joint seals reliably. The surface pressure on the gasket is limited downwards by the

leakage of the joint and upwards by the strength of the gasket. It is crucial that the surface pressure is evenly distributed over the surface of the gasket. An uneven load on the gasket leads to places where the gasket is overloaded and places with insufficient pressure where the joint can leak. Investigations of flange joints with gaskets [50,51] deal with the stress on the connecting elements (flange, gasket, bolt) and analyse the leakage of the joint at different preloads.

For flange joints of steel structures, the clamping force has a further significance. For joints that also transmit transverse or shear forces, the clamping force is the normal force that provides friction on the contact surfaces. If the clamping force is missing, the working load is transferred directly to the bolts, which leads to elongation of the bolts and the formation of a gap between the flanges. The force–displacement diagram in Figure 1 provides a good overview of the situation in the bolted joint when the working load is applied to the bolt axis. The additional load on the bolt is independent of the preload as long as there is at least a minimum clamping force between the clamping parts. The effect of the preload on the additional load in the bolt is shown in the diagrams in Figure 14. If there is no clamping force between the coupling parts, the entire increase in the working load is transferred to the bolt (Figure 14b).

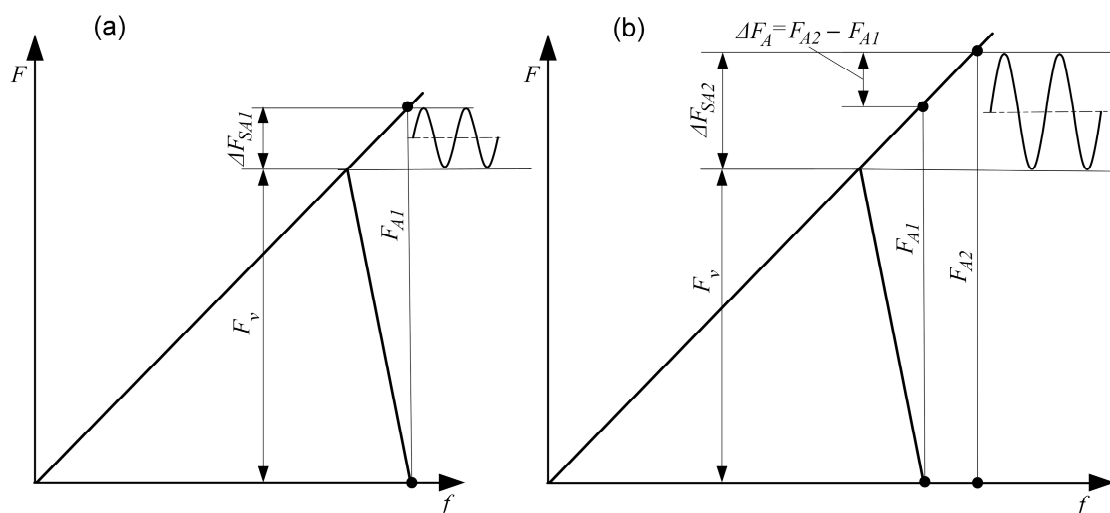


**Figure 14.** Effect of preload on the additional load in the bolt: (a) the limit case when the clamping force just drops to zero due to the working load, and (b) the case when the working force is further increased.

Due to the eccentric action of the working load, the preload relieves the clamping parts at the edge of the flange, i.e., on the side from which the working load is applied. With a higher preload, the opening of the joint occurs at a higher working load. Slecza and Len [52] analytically discuss the opening of a flange joint and the influences that affect the opening. Ajaei and Soyoz [53] analyse the effect of bolt preload on the fatigue of bolts in the flanges of a wind turbine tower. The results of their numerical analyses show that the preload affects the magnitude of the bending stress in the bolt and the fatigue life of the bolt. A general conclusion from several studies is that a higher preload leads to a higher mean stress in the bolt but a lower amplitude stress, which is crucial for the fatigue of the bolt. It is essential that the preload does not exceed the yield strength of the bolt.

Knowing the clamping force, the working load, and the additional load on the bolt, the required preload can be estimated analytically as follows:

$$F_{Vmin} = F_{KL} + F_A - F_{SA} + F_Z \quad (9)$$

Due to the plastic deformation of uneven contact surfaces, the preload decreases by  $F_Z$  after a certain number of load repetitions. VDI 2230 [17] provides an equation for

calculating the settlements as a function of the roughness of the contact surfaces. The total settlement  $f_z$  depends on the roughness parameters and the number of contact surfaces.

$$F_Z = \frac{f_z}{(\delta_S + \delta_P)} \quad (10)$$

The bolt preload  $F_V$  is commonly achieved by tightening the nut or the bolt with the specified torque ( $M_A$ ). Tightening involves overcoming friction on two separate surfaces: between the threads ( $M_G$ ) and under the nut or bolt head ( $M_{KR}$ ). The torque  $M_A$  required to achieve the desired preload  $F_V$  can be analytically calculated using Equation (11).

$$M_A = M_G + M_{KR} = F_V \cdot \tan(\varphi + \rho') + F_V \cdot \frac{D_{Km}}{2} \cdot \mu_K \quad (11)$$

For a metric ISO thread with a thread profile angle of  $60^\circ$ , Equation (11) can be rearranged and written as follows [19]:

$$M_A = F_V \cdot \left( 0.175 \cdot P + 0.577 \cdot d_2 \cdot \mu_G + \frac{D_{Km}}{2} \cdot \mu_K \right) \quad (12)$$

The standard clearly defines geometric parameters such as the thread pitch  $P$ , the pitch diameter  $d_2$ , and the mean diameter of the circular ring under the bolt head  $D_{Km}$ . The coefficients of friction between the threads  $\mu_G$  and under the bolt head or nut  $\mu_K$  are not easy to define. A range of friction coefficients are given in the literature for certain tribological conditions. Croccolo et al. [54] have discussed the influence of surface finish, lubrication, and the effect of repeated tightening on the coefficient of friction between the threads. Liu et al. [55] investigate the influence of surface topography and surface inclination on the coefficient of friction in bolted joints. By analysing the micro-level interactions between the surfaces, they derive an analytical model to calculate the coefficient of friction, which is dependent on the parameters of surface roughness and contact load. As the contact load increases, the actual contact area also increases. The coefficient of friction initially rises with increasing contact load until it reaches a threshold value, beyond which it remains constant.

For rolled threads that are galvanised and lubricated, the coefficient of friction is between 0.1 and 0.18 [19]. If the maximum value is used when specifying the required torque and the coefficient of friction is at the lower limit during assembly, the preload of the bolted joint would be too high, possibly resulting in a stress higher than the yield strength.

VDI 2230 recommends that the minimum coefficients of friction and the maximum installation force  $F_M = F_{Vmax}$  (which takes into account the tightening coefficient  $\alpha_A$  to account for the scatter in tightening) are taken into account when specifying the required tightening torque  $M_A$ . For tightening with torque wrenches, it is recommended that  $\alpha_A = 1.4$ – $1.8$ .

$$F_M = F_{Vmax} = \alpha_A \cdot F_{Vmin} \quad (13)$$

For flange joints of steel structures, it is desirable to keep the preload as high as possible during installation. Therefore, in most cases, high-strength bolts with a strength class of 10.9 and a yield strength of about 900 MPa are used. Several authors [37–39] in the technical and scientific literature recommend preloading bolts up to 70% of the bolt yield strength. The surface pressure between the bolt head or nut and the flange surface can also be problematic. There is a risk of the head of the bolt or nut pressing into the softer surface of the clamping parts. When evaluating a bolted joint, the surface pressure should be calculated and compared with the permissible values from the literature [19]. High-strength bolt sets (HV-sets) include, in addition to the bolt and nut by the EN 14399-4 [56], two washers by EN 14399-6 [57]. Compared to bolts by ISO 4014 [58] and nuts by ISO 4032 [59], they have a larger wrench size and a larger washer outer diameter for the same nominal bolt diameter. This increases the loading surface and reduces the surface pressure between the bolt head or nut and the clamping parts. In the case of IHF kits, per Recommendation Z-14.4-800 [60], the nut and bolt head are already designed to have a larger contact area with the flange

than a conventional bolt and nut. This kind of bolt designs are used when surface pressure is causing issues with the standard bolts by ISO 4014.

When the preload is defined, it must be applied during installation. The value of the preload achieved is determined indirectly by measuring one of the following quantities: tightening torque  $M_A$  (usually with a torque wrench), nut or bolt rotation  $\theta$ , bolt elongation  $f_S$ , gradient  $dM_A/d\theta$ , magnitude of the impulse during motorised tightening, and pressure during hydraulic tightening. Due to the indirect measurement of the preload, there can be significant differences between the desired and actual values. The differences depend on the tightening method used. An explanation of the methods and an analysis of the scatter is given in [19] and VDI 2230 [17]. Two methods are highlighted here: preload measurement via the tightening torque and hydraulic tightening, which is mainly used when tightening bolts with a large diameter.

When tightening a bolt with a torque wrench, the desired torque is set on the torque wrench. The tables in [19] provide information on the maximum permissible tightening torque for a specific bolt diameter, a specific bolt strength class, and a specific coefficient of friction. If the tightening torque is below the specified limit, the stress acting on the bolt will not exceed 90% of the yield strength of the bolt. The problem arises when the coefficient of friction has to be estimated. To be on the safe side, it is recommended to select the torque with the lowest possible coefficient of friction. When checking the torque with a torque wrench, the preload scatter is estimated at  $\pm 23$ – $28\%$  [19]. The scatter of the coefficient of friction has the dominant influence, and a high-precision torque wrench does not significantly improve the overall scatter.

During hydraulic tightening, an axial force is applied to the bolt at the free end, which causes an elongation of the bolt and the formation of a gap between the nut and the clamping parts [61]. In the next step, the nut is screwed to the clamping parts. After the pressure in the hydraulic bolt tensioning device (HBT) has been released, the bolt presses the clamping parts together with a preloading force. Due to the elastic and plastic deformation of the clamping parts, the actual preload is lower than the axial force applied to the bolt using HBT. The difference is greater if the ratio of bolt length to bolt diameter  $l/d$  is smaller. According to [19], the scatter is up to  $\pm 23\%$  for  $l/d < 5$  and up to  $\pm 10\%$  for  $l/d > 5$ . The recommended tightening coefficients are  $\alpha_A = 1.6$  in the first case and  $\alpha_A = 1.2$  in the second case.

Differences between the desired and actual preload also arise due to the elastic interaction between the bolts during tightening. When a bolt is preloaded, the elastic deformation of the clamping parts reduces the preload in other bolts. The influence of elastic interactions on the preload scatter can be reduced by selecting an appropriate tightening sequence. Based on analytical, numerical, and experimental studies, various tightening patterns have been proposed in the technical and scientific literature [62–68]. One of the most commonly used is the multi-stage cross-tightening. The elastic interaction between individual bolts can be avoided by tightening the bolts simultaneously. The method is limited to a small number of bolts and simple joint geometries. This type of tightening requires customised equipment (e.g., simultaneous use of several HBTs).

A comprehensive overview of the literature on screw-tightening techniques and sequences is given by Croccolo et al. [69] in a review article. In bolted joints that are exposed to vibrations, there is a risk of the bolts loosening and the preload decreasing. In extreme cases, the connection can even be damaged if the bolt fails. The problem of loosening is dealt with by Croccolo et al. [70] in a review paper, which also contains an extensive bibliography on this topic.

## 6. Effect of Geometric Imperfections on Bolt Fatigue

Most analyses of preloaded bolted joints are performed for geometrically ideal flange shapes and contact surfaces. Such an analysis was also performed in our previous study [27]. The flange contact surfaces were ground and therefore ideally flat. The finite element method was used to determine the additional loads in the bolts and the stress levels at

different working loads. A progressive dependence of the bolt's additional load on the working load was obtained in all analyses. The results of the numerical analyses were verified by tests. The measurements were also carried out on non-ground flanges. Since considerable discrepancies were found between the experimental and numerical results, we decided to grind the contact surfaces of the flanges and, on the other hand, to carry out a thorough examination of the flanges with imperfections. At the end of this section, only some of the most important results of our research are presented together with comments, while the comprehensive overview with all the details is presented in [71].

In reviewing scientific papers on flange joint imperfections from the last 25 years, we have found that researchers have mainly focused on large flanges. These are used in wind turbine towers. The researchers found that the unevenness of the contact surfaces significantly affects the magnitude of the additional load on the bolt, which in turn has a major impact on the fatigue of the preloaded bolts. Large flanges are welded to the pipe, but the contact surfaces are not machined after welding. A gap forms at the flange contact, which affects the additional load on the bolt at the gap location. If the gap is small and the flange is sufficiently elastic, the gap may close during preloading, but the additional load on the bolt is still greater than the theoretical load. Jakubowski [72] classified the flange imperfections in the case of wind turbine towers into three basic groups: the conical gap on the tower side of the joint (on the outside of the tower tube), the conical gap on the flange side (on the inside of the tower tube), and the parallel gap under the bolts. He found that the critical imperfections are the gap on the tower side, where the working load is applied, and the parallel gap. In both cases, the additional bolt loads are significantly higher than with ideal flanges. Other researchers [73,74] have also come to the same conclusions. The recommended tolerances for wind turbine flanges were determined on the basis of theoretical studies and experience. Seidl has compiled guidelines from various sources and his research results [75]. The upper limit for the gap height is around 2 mm. Feldmann et al. [76] studied two correction methods to reduce the influence of imperfections on the fluctuating load on the bolts. They used 0.5 mm-thick inserts and inserted them into the gaps under the bolts. The number of inserts depended on the height of the gap under each bolt. In Method 1, the bolts were first tightened to 50% of the intended preload and then the required number of inserts were inserted. In Method 2, the bolts were tightened to only 10% of the preload before the inserts were fitted. The forces in the bolts were determined experimentally for the ideal geometry, the geometry with a maximum gap of 7 mm, and the forces after corrections. Significantly better results were achieved with Method 2, as the values of the additional forces in the bolts approached those of the flanges without imperfections. When using Method 1, the additional forces in the bolts in the middle of the working load range were reduced by around 50%.

The finite element method is increasingly being used to determine forces and stresses in bolts. For large flanges, the analysis is reduced to the connection of two L-segments connected by a bolt. Tran et al. numerically analysed the effects of gap depth on the stress situation in the bolts in a 5 MW wind turbine [77]. They found that the critical gap is on the tower side and the stress in the bolts increases with increasing gap depth. Seidl et al. [78] used the finite element method to determine the relationship between the loads acting on the tower segments and the stresses in the bolts. The measured values of the flange imperfections were included in the analysis. The results were compared with the results of measurements carried out on the wind turbine in 2001 and documented in the test report. The study showed good agreement between the numerical analysis and the measurement results. More recent experimental results were presented by Weijtjens et al. [79], who carried out measurements on offshore wind turbines as part of a research project between 2017 and 2020. Measuring bolts were installed on three turbines on which strain gauges were also glued to the tower above the bolts to measure the strain in the segment. The ratio between the force in the bolt and the force on the segment (working load) was determined for various load conditions and referred to as the Load Transfer Function (LTF). In parallel, the joint was analysed (including the flange inclination) using the finite element method



(FEA). The study showed good agreement between the measured results and the results obtained by the FEA.

In our research [71], we have investigated the influence of geometric imperfections on the additional load in the bolt for small flanges. Experimental and numerical investigations confirmed the tendencies observed in large flanges. We studied the two flange joints shown in Figure 5. Using inclined/conical inserts, we simulated a gap between the flanges (Figure 15) of only 0.02 to 0.03 mm. The study showed that even minimal flange unevenness, which is always present without special precision machining, significantly affects the conditions in the bolted joint considerably. The results of the measurements are shown in Figure 16. The joints were also analysed using the finite element method and comparable results were obtained.

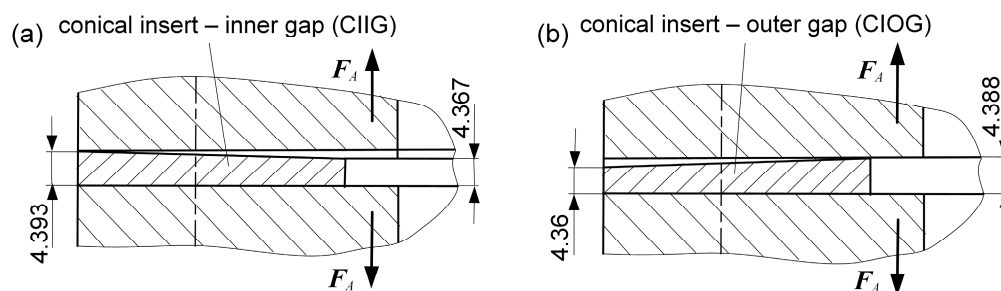


**Figure 15.** Simulation of flange joint imperfections with an inclined insert: (a) gap on the side of working force application and (b) gap on the opposite side of the working force application; Reprinted with permission from ref. [71]. Copyright (2024), with permission from Elsevier.

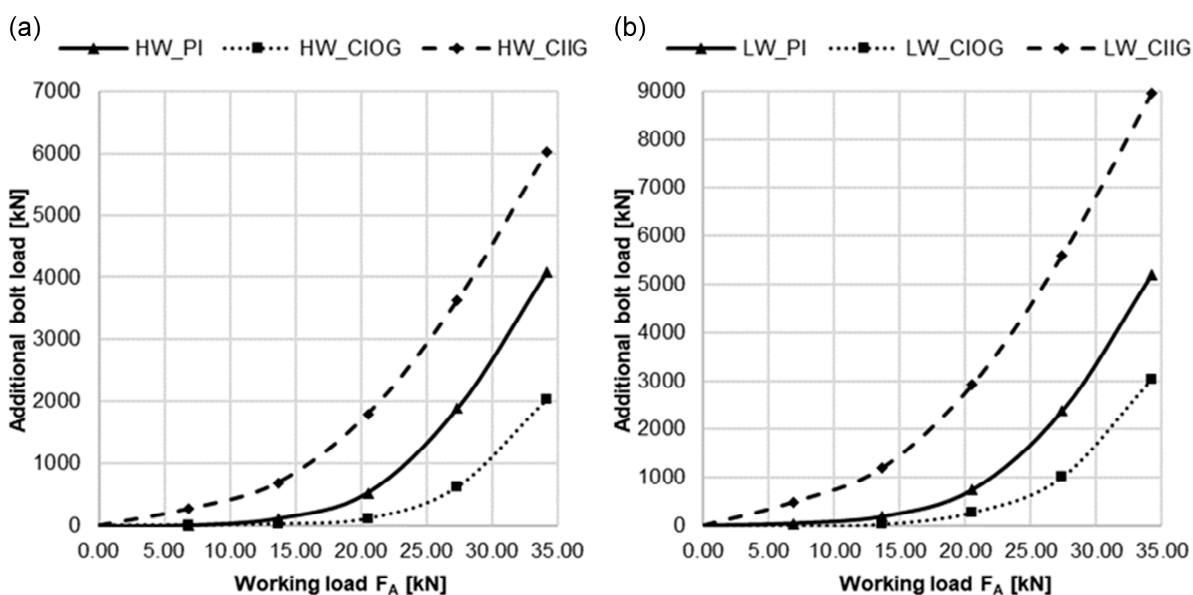


**Figure 16.** Additional bolt load: (a) in a high washer joint (HW) and (b) in a standard washer joint (LW); Reprinted with permission from ref. [71]. Copyright (2024), with permission from Elsevier.

The results evidently show that the gap on the inside (CIIG case) has a negative effect on the additional load in the bolt, which is therefore much higher than in the case of the ideal insert. On the other hand, the gap on the outside reduces the additional load in the bolt compared to the case of the ideal insert. The same effect can be observed when using long and short bolts or high and standard washers. Figure 16 compares the effect of flange imperfections for long and short bolts. It can be seen that the long bolt in the ideal joint has a lower additional load, and the load on the long bolt is also significantly lower in the case of the uneven flange, which is to be expected since a more elastic bolt is used, which has

long been a well-known solution for reducing the fluctuating load on bolts. To mitigate the deleterious effects of these imperfections, the proposal and evaluation of employing filler material between the flanges are presented as well. Specifically, it is demonstrated that a thin layer of liquid metal filler (Kemiskit Fe21) substantially decreased the alternating load on bolts. Empirical findings illustrate that this corrective measure enhances the fatigue life of bolts by a factor of more than 30 under the highest applied working load condition. A quantitative example which clearly shows the effect of geometric imperfections on bolt fatigue is shown in Appendix A.4 (see Figure A4 and Table A4).

## 7. Fatigue Durability of Bolts

A bolt is a typical machine element in which high local stress concentrations occur due to geometric variations along the length of the bolt. Several sources [19,80,81] state that 65% of fractures occur at the contact between nut and bolt, 20% at the transition between thread and shank, and 15% at the transition between bolt and head. Standard bolt shapes, nut shapes, and thread shapes are not optimal from the point of view of the notch effect but are still commonly used in practical applications.

Once the stress amplitude in the bolt  $\sigma_A$  or the stress range  $\Delta\sigma_R$  is known, the number of load repetitions until bolt failure can be determined. S-N curves are required to determine the fatigue life. S-N curves for standard test specimens exist for various materials, including the materials from which the bolts are made. By taking into account the notch effect and other additional influences (cross-section size, thread manufacturing process, surface protection), an S-N curve for the bolt can be determined. Welch [82] used this method to determine S-N curves in his study on bolt fatigue. This method is rarely used in practise. In most cases, S-N curves based on tests of bolts under axial load are used to evaluate the fatigue of bolts. Numerous results of dynamic tests of bolts are available in the technical and scientific literature [46,47,81,83,84]. The bolt load is characterised by high mean stress and (by comparison) very low amplitude stress. Due to the sharp notch and the consequent high stress concentration, the fatigue life of bolts is, in most cases, hardly affected by the mean stress or the bolt material. It is only important that the bolt yield strength is not exceeded during preloading. In most guidelines, including Eurocode 3 (EN 1993-1-9), the influence of mean stress is neglected.

In the Eurocode 3 classification, tension-loaded bolts belong to the detail category 50. The S-N curve for detail 50 ( $\Delta\sigma_C = 50$  MPa) is shown in Figure 17 and described by Equation (13). The slope of the curve is  $m = 3$  up to  $10^6$  cycles, and  $m = 5$  above  $10^6$  cycles. The detail applies to both cut and rolled threads.

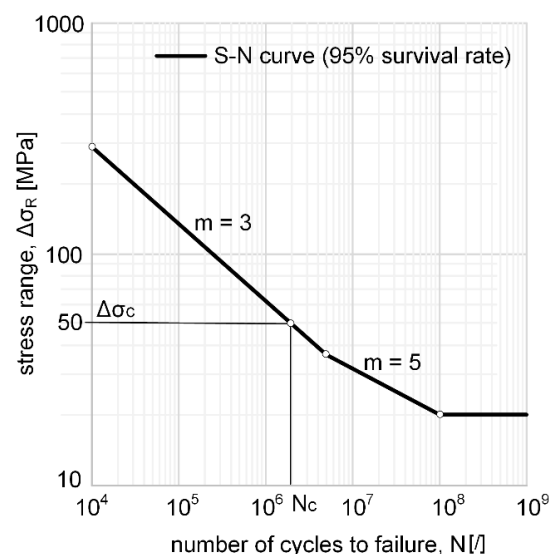


Figure 17. S-N curve for detail 50 as per Eurocode 3.

$$\Delta\sigma_R^m \cdot N_R = \Delta\sigma_C^m \cdot 2 \cdot 10^6 \quad (14)$$

For bolt diameters above 30 mm, the reduced values must be used.

$$\Delta\sigma_{Cred} = k_s \cdot \Delta\sigma_C \quad (15)$$

$$k_s = \left( \frac{30\text{mm}}{d} \right)^{0.25} \quad (16)$$

According to the EN 13001-3-1 standard [85], three different detail categories can be used for tension-loaded bolts in crane construction: detail 50 for cut threads, detail 63 for bolts with rolled threads larger than M30, and detail 71 for bolts with rolled threads M30 or smaller. An overview of S-N curves used in other standards is given by Maljaars and Euler in [86].

The evaluation of high-strength bolts of classes 8.8–12.9 for general engineering applications is dealt with in the VDI 2230 guideline. Instead of the stress range, the stress amplitude  $\sigma_A$  is used to determine the bolt fatigue life. For bolts that are heat-treated after rolling the thread (SV), the stress amplitude is determined by the following equation:

$$\sigma_{ASV} = 0.85 \cdot \left( \frac{150}{d} + 45 \right) \quad (17)$$

Bolts that are heat-treated before the thread is rolled (SG) have a higher fatigue strength. In the following equation,  $F_{Sm}$  is the mean load in the bolt, and  $F_{0.2min}$  is the load at which the bolt yield strength is reached.

$$\sigma_{ASG} = \left( 2 - \frac{F_{Sm}}{F_{0.2min}} \right) \cdot \sigma_{ASV} \quad (18)$$

The guideline also states that the values are about 20% lower if the bolts are hot-dip galvanised.

The shape of the S-N curve is influenced by several parameters, which are briefly explained below. The shape of the bolt elements (nut, bolt, thread), the size of the bolt cross-section, the thread manufacturing procedure, and the surface condition of the bolt all influence the fatigue strength of the bolt.

The first measure to increase the fatigue strength of a bolt is to reduce the notch effect in critical areas. In most joints, a standard nut is used where most of the load is applied to the first few threads. The notch effect coefficient, which describes the increase in the nominal stress, is between four and five [82] on the first thread in the nut. Due to the high stress concentration, most fractures occur on the first load-bearing thread. More elastic nuts, or grooves in the bolt, ensure a more even distribution of the load on the threads and thus reduce the notch effect [87–89]. One possibility for distributing the load more evenly across the threads is to vary the thread pitch along the height of the nut [90–92]. Standard threads have the bottom of the thread rounded with an arc, which is not an optimal solution but is nevertheless used in most practical applications. Solutions to reduce the notch effect at the transition between the thread and the bolt shank are presented in [93]. Optimising the transition curve can reduce the notch effect at the bolt head [94].

The fatigue strength of machine elements decreases as their cross-section increases. This phenomenon is taken into account in Eurocode 3 and VDI 2230. The power of wind turbines has increased over the last twenty years, and so has the size of all components, including bolts. Research on the effect of large bolt diameters (up to M72) on fatigue life has been most intensive in this area in recent years. Researchers have found [84] that the reduction in load-carrying capacity is less than predicted in Equation (16).

The fatigue strength of bolts is influenced by the threading process. Threads can be produced by cutting or rolling. Rolling creates residual compressive stresses at the root of the thread, which increase the load-bearing capacity of the bolts [95,96]. It is also

important whether rolling is carried out before or after heat treatment. If the bolts are heat-treated after rolling, the compressive stresses are relieved and the positive effect on fatigue is significantly reduced. Bolts in steel structures are protected against corrosion—most commonly by hot-dip galvanising. Experimental studies by several researchers [47,84] show that hot-dip galvanising reduces the fatigue resistance of bolts by around 20–25%.

## 8. Conclusions

This paper aims to provide a compact overview of the effects which influence the fatigue life of dynamically loaded prestressed bolted joints. It is essential to be aware of these effects and to consider them in design, installation, and maintenance. The effects on the fatigue life of bolts are interwoven and require a holistic approach. The bolt fatigue life depends on the durability of the bolt (material, design, manufacturing, etc.), on the one hand, and on the stress state in the bolt, on the other hand. The determination of the actual stress situation in the bolt poses the most significant challenge in the evaluation of bolts regarding fatigue.

Analytical methods developed before the widespread use of the finite element method are relatively conservative and, therefore, on the safe side. An example of such a method is the Schmidt–Neuper method for determining the additional load in a bolt. Among the best-known analytical methods is the VDI 2230 calculation, which also takes into account the influence of the point of action of the working load in the joint. This method is very accurate for simple joints, whereas it is difficult to determine some parameters for the joints from practical use.

Recently, FEM analysis has been increasingly used to determine the exact loads in prestressed bolts, which has been proven to provide very good results and enable optimisation of the flange bolting. Due to the desire to optimise material consumption and thus reduce weight, which is a recent trend, premature failure of bolts is occurring more than in the past. This is due to the lack of knowledge of the exact values of certain parameters (e.g., coefficient of friction, geometric imperfections of the flanges, or actual preload) which can change the realistic conditions that are not taken into account in the FEM analysis or other calculations. Therefore, a certain safety factor must always be taken into account when determining the size and type of bolts and their preload. The more accurately someone can estimate or determine all the influencing parameters of the joint, the lower the safety factor can be.

One single factor that has a major impact on the other influences on fatigue is preload. In the first place, preloading is important because of the risk of bolt loosening and damaging the joint due to the bolt failure. From a fatigue point of view, a high preload ensures a constant clamping force and reduces the influence of bending on the additional load of the bolt. A high preload can also reduce the influence of geometric imperfections on the bolt's additional load. Due to the indirect measurement of the preload and the elastic interactions between the bolts, the desired preload may differ significantly from the actual preload, even if the installation is carried out professionally in accordance with the instructions. Incorrect installation will result in significant differences between the load on individual bolts and consequently the breakage of the bolts with the highest magnitude of fluctuating load (the ones with the lowest preload in the case of uniform distribution of working load among the bolts).

For the need to optimise or define the prestressed flange joint, which is not based on large safety factors and therefore possibly oversized, it is necessary to know precisely all the parameters that influence the fatigue life of the bolt. In order to avoid situations that can lead to the failure of a single bolt or even the entire bolted connection, the influencing parameters and variables should be briefly summarised:

- Fatigue strength: We generally have no influence on this part, except for special requirements when we decide to use non-standardised bolts. For standardised bolts we rely on measurements on bolts whose S-N curves are known. If we want to optimise the size of the bolt and its fatigue strength, we must take into account the

heat treatment and the manufacturing process of the bolt so that we can choose a suitable S-N curve;

- Preload force magnitude: As described in the article, there is a general consensus that the greater the preload force of the bolt, the lower the additional load on the bolt. Of course, care must be taken to ensure that the maximum stress (at the time the working force is applied) in the bolt does not exceed the yield strength. In general, the recommended preload of bolts is up to 70% of the bolt yield strength. In order to be able to reliably determine the maximum force in the bolt when applying the working load, we must also take into account the other parameters, which are described in more detail below. Another factor that must be taken into account when determining the preload force is the difference between the specified and the actual preload force. In order to bring the actual preload as close as possible to the desired preload, the method of tightening or preload force control must be adjusted. Tightening with a torque wrench is the least accurate method, so in critical cases it is better to use tightening based on measuring bolt elongation, either directly or indirectly by monitoring the rotation of the nut, or tightening using the hydraulic elongation of the bolts, as described in this article;
- Resilience of bolt and clamping parts: Precise knowledge of the resilience of bolts and clamping parts is important for the analytical determination of the additional load on bolts. In general, the lower the resilience of the bolt and the higher the resilience of the clamping parts, the lower the additional load on the bolt;
- Point of action of the working load: The additional load on a preloaded bolt when it is subjected to a working load depends on the point of action of the working load. Theoretically, the point of action of the working load is very difficult to determine precisely. It is recommended to design the flange joint so that the point of action of the working load is as close as possible to the bolt axis and directly under the bolt head. The first measure prevents bending stresses from being introduced into the bolt, and the second enables the entire clamping parts to be relieved when the working load is applied. Both measures reduce the value of the additional force on the bolt and thus increase its fatigue life;
- Point of action of the working load: The additional load on a preloaded bolt when it is subjected to a working load depends on the point of action of the working load. Theoretically, the point of action of the working load is very difficult to determine precisely. It is recommended that the flange connection is designed so that the point of action of the working load is as close as possible to the bolt axis. This prevents bending stresses from being introduced into the bolt, which reduces the value of the additional force on the bolt and thus increases its fatigue life;
- Working load distribution: analytically, it is practically impossible to predict the distribution of the working load on the bolts in flange joints with absolute accuracy when the working load is not applied symmetrically to the bolts. If the exact geometry is known, it is shown that the FEM analysis allows a very accurate determination of the distribution of the working load on the bolts and is recommended for evaluation in critical cases;
- Geometric imperfections: As described in many publications, geometric imperfections have a significant impact on the fatigue life of preloaded bolts in flange joints. Since the point of action of the working load is usually eccentric to the bolt axis, the geometric imperfections that cause gaps between the flanges on the side from which the working load is applied are critical. It has also been shown that with smaller flanges, even gaps of a few hundredths of a millimetre are problematic. To avoid this problem, it is advisable to design the flange surfaces so that the gap is always present on the opposite side from which the working load is applied, which has a positive effect on the fluctuating load on the bolt and thus on its fatigue life.

Based on a review of the existing literature and our own experience, we observe that the individual factors influencing bolt fatigue have already been extensively researched,

making it difficult to define guidelines for further studies. However, a promising area for future research is the investigation of corrective measures to address geometric irregularities in bolted joints. Recent cases, such as the failure of bolted joints in wind turbine support columns, show the importance of these irregularities. Studies have shown that the dynamic loading of prestressed bolts can be significantly reduced by using appropriate fillers to compensate for gaps caused by geometric irregularities [76]. Progress in this area could be achieved by developing a filler that can be easily introduced into the joints, as shown by Okorn et al. for small flanges [71]. Including the topography of real contact surfaces in this research would also be beneficial.

**Author Contributions:** Conceptualization, I.O., M.N., J.K. and S.O.; methodology, I.O., M.N., J.K. and S.O.; validation, I.O., M.N., J.K. and S.O.; investigation, I.O., M.N., J.K. and S.O.; resources, I.O., M.N., J.K. and S.O.; data curation, I.O., M.N., J.K. and S.O.; writing—original draft preparation, I.O. and S.O.; writing—review and editing, I.O., M.N., J.K. and S.O.; visualization, I.O. and S.O.; supervision, M.N., J.K. and S.O.; project administration, M.N., J.K. and S.O.; funding acquisition, M.N. and J.K. All authors have read and agreed to the published version of the manuscript.

**Funding:** This research was funded by the SLOVENIAN RESEARCH AGENCY, grant number P2-0182 entitled Development Evaluation.

**Data Availability Statement:** The raw data supporting the conclusions of this article will be made available by the authors on request.

**Conflicts of Interest:** The authors declare no conflicts of interest.

### Appendix A. Quantitative Comparisons of Different Influences on the Fatigue Life of the Bolt for Selected Cases

Appendix A.1. Influence of Resilience of Bolt and Clamping Parts on Bolt Fatigue (A Summary of Results from [27] is Presented)

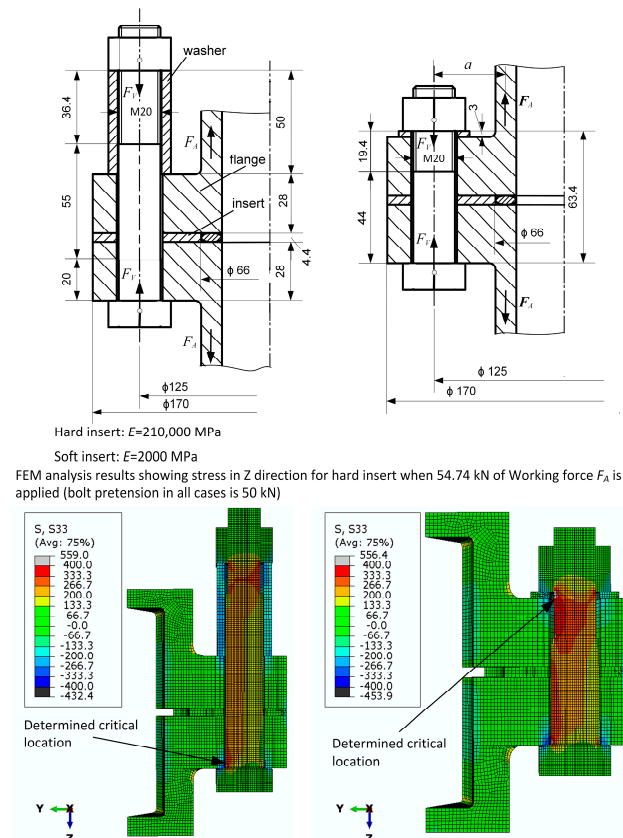


**Figure A1.** Examples discussed to demonstrate the influence of resilience of bolt and clamping parts on bolt fatigue; Adapted from ref. [27].

**Table A1.** Fatigue life assessment of the bolt for numerically gained (FEM) stress ranges (number of cycles to failure).

Geometry	Working Load $F_A$ [kN]							
	6.84	13.68	20.53	27.37	34.2	41.05	47.89	54.74
HW-HI	INF	INF	INF	INF	$5.78 \times 10^6$	$1.35 \times 10^6$	$4.94 \times 10^5$	$2.58 \times 10^5$
HW-SI	INF	INF	$2.78 \times 10^7$	$4.59 \times 10^6$	$1.91 \times 10^6$	$8.84 \times 10^5$	$4.35 \times 10^5$	$2.66 \times 10^5$
LW-HI	INF	INF	INF	$2.52 \times 10^7$	$1.76 \times 10^6$	$4.62 \times 10^5$	$1.73 \times 10^5$	$8.6 \times 10^4$
LW-SI	INF	$4.47 \times 10^7$	$3.86 \times 10^6$	$1.23 \times 10^6$	$4.98 \times 10^5$	$2.45 \times 10^5$	$1.29 \times 10^5$	$7.18 \times 10^4$

Note: HW—high washer or long bolt, LW—low washer or short bolt, HI—hard insert, SI—soft insert.

*Appendix A.2. Influence of the Point of Action of the Working Load on Bolt Fatigue*

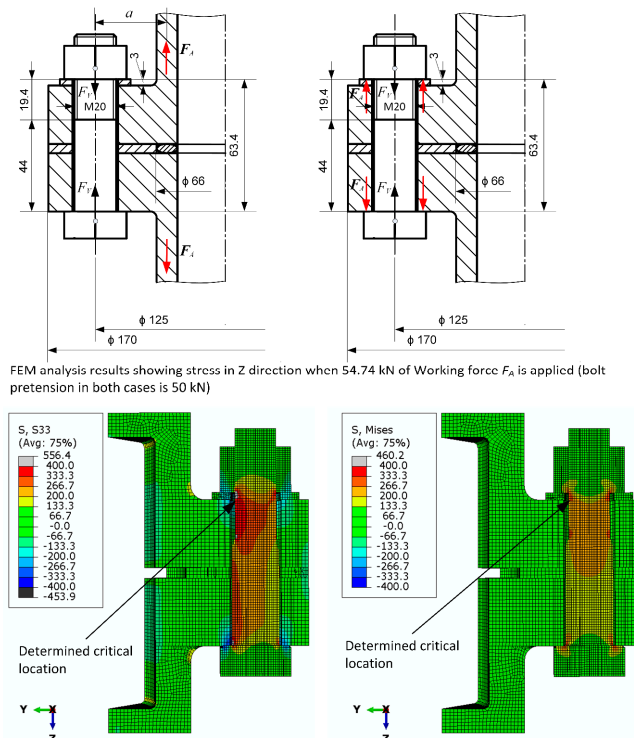


**Figure A2.** Examples discussed to demonstrate the influence of the point of action of the working load on bolt fatigue.

**Table A2.** Fatigue life assessment of the bolt for numerically gained (FEM) stress ranges (number of cycles to failure).

WL App. Loc.	Working Load $F_A$ [kN]							
	6.84	13.68	20.53	27.37	34.2	41.05	47.89	54.74
Eccentric $a = 27.5$ mm	INF	INF	INF	$2.52 \times 10^7$	$1.76 \times 10^6$	$4.62 \times 10^5$	$1.73 \times 10^5$	$8.06 \times 10^4$
Centric	INF	INF	INF	$3.45 \times 10^7$	$8.39 \times 10^6$	$4.93 \times 10^6$	$3.09 \times 10^6$	$1.98 \times 10^6$

Appendix A.3. Working Force Distribution (A Summary of Results from [13] is Presented)

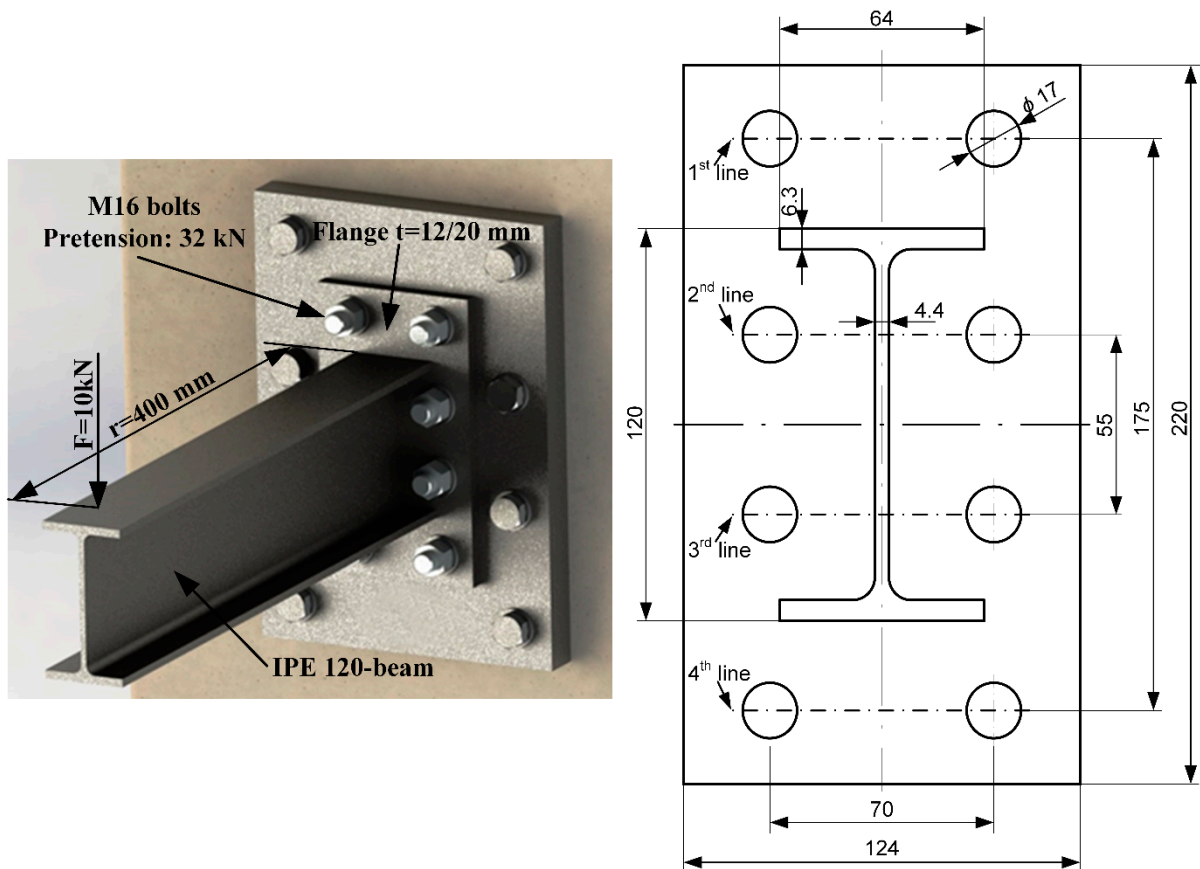


Figure A3. Cantilever beam connection example to demonstrate the working force distribution among pretensioned bolts; Adapted from ref. [13].

Table A3. Comparison of the calculated working force on bolts using different analytical methods, FEM analysis, and measurement.

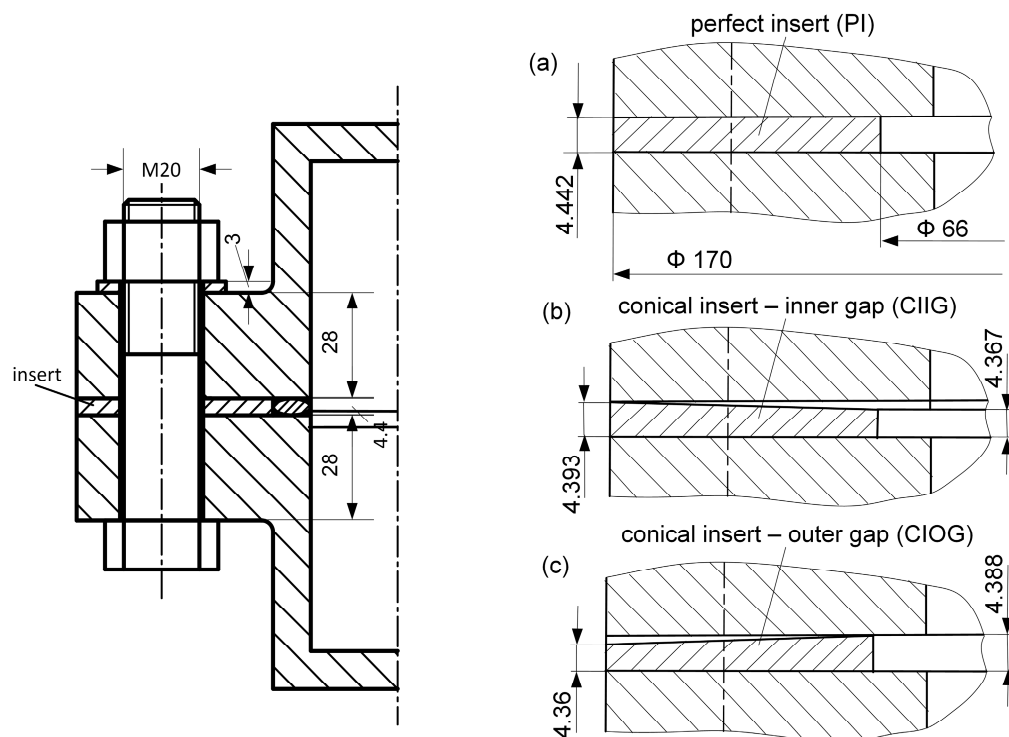
Analysis 1: I-Beam, Flange Thickness = 12 mm								
Working Load [N] on Bolts at:	Calculation Method						FEM Analysis	Measurement
	Kržič	Hamrock	Matek	Aghayere	Oman			
1st line	8795.1	6056.0	10,226.5	7567.5	7670.4	8922.1	6725	
2nd line	8795.1	4216.2	5920.6	4650.3	10,867.1	11,163.5	11,055	
3rd line	-8795.1	2529.7	1973.5	1976.2	0.0	-61.5	1190	
4th line	-8795.1	689.9	-2332.4	-940.9	0.0	-24.6	830	

Analysis 2: I-Beam, Flange Thickness = 20 mm							
Operational Force [N] on Bolts at:	Calculation Method						FEM Analysis
	Kržič	Hamrock	Matek	Aghayere	Oman		
1st line	8795.1	6056.0	10,226.5	7567.5	7512.2	8761.2	
2nd line	8795.1	4216.2	5920.6	4650.3	10,643.0	10,825.9	
3rd line	-8795.1	2529.7	1973.5	1976.2	0.0	-1556.6	
4th line	-8795.1	689.9	-2332.4	-940.9	0.0	-973.3	



Appendix A.4. Influence of Geometric Imperfections on Bolt Fatigue (A Summary of Results from [71] is Presented)



**Figure A4.** Examples discussed to demonstrate the influence of geometric imperfections on bolt fatigue: (a) joint with perfect contact, (b) joint with conical gap in the inner side and (c) joint with conical gap on the outer side; Adapted from ref. [71].

**Table A4.** Fatigue life assessment of the bolt for numerically gained (FEM) stress ranges (number of cycles to failure).

Geometry	Working Load $F_A$ [kN]							
	10.26	13.68	17.09	20.51	23.93	27.35	30.77	34.2
LW-PI	INF	INF	INF	INF	INF	$2.16 \times 10^7$	$3.90 \times 10^6$	$1.58 \times 10^6$
LW-CIIG	INF	INF	INF	$4.53 \times 10^7$	$6.37 \times 10^6$	$2.24 \times 10^6$	$1.03 \times 10^6$	$5.42 \times 10^5$
LW-CIOG	INF	INF	INF	INF	INF	INF	INF	$1.19 \times 10^7$

## References

- Jaszak, P.; Adamek, K. Design and analysis of the flange-bolted joint with respect to required tightness and strength. *Open Eng.* **2019**, *9*, 338–349. [\[CrossRef\]](#)
- Abid, M.; Nash, D.H.; Javed, S.; Wajid, H.A. Performance of a gasket joint under bolt up and combined pressure, axial and thermal loading—FEA study. *Int. J. Press. Vessel. Pip.* **2018**, *168*, 166–173. [\[CrossRef\]](#)
- Van-Long, H.; Jean-Pierre, J.; Jean-François, D. Behaviour of bolted flange joints in tubular structures under monotonic, repeated and fatigue loadings I: Experimental tests. *J. Constr. Steel Res.* **2013**, *85*, 1–11. [\[CrossRef\]](#)
- Pavlović, M.; Heistermann, C.; Veljković, M.; Pak, D.; Feldmann, M.; Rebelo, C.; daSilva, L.S. Friction connection vs. ring flange connection in steel towers for wind converters. *Eng. Struct.* **2015**, *98*, 151–162. [\[CrossRef\]](#)
- Lochana, S.; Mehmanparasta, A.; Wintle, J. A review of fatigue performance of bolted connections in offshore wind turbines. *Procedia Struct. Integr.* **2019**, *17*, 276–283. [\[CrossRef\]](#)
- Schaumann, P.; Böhm, M.; Schürmann, K. Improvements in the fatigue design of support structures for offshore wind turbines. *Steel Constr.* **2021**, *14*, 74–82. [\[CrossRef\]](#)
- Mehmanparast, A.; Lotfian, S.; Vipin, S.-P. A Review of challenges and opportunities associated with bolted flange connections in the offshore wind industry. *Metals* **2020**, *10*, 732. [\[CrossRef\]](#)
- Rincón-Casado, A.; Juliá-Lerma, J.-M.; García-Vallejo, D.; Domínguez, J. Experimental estimation of the residual fatigue life of in-service wind turbine bolts. *Eng. Fail. Anal.* **2022**, *141*, 106658. [\[CrossRef\]](#)

9. Deng, H.-Z.; Li, C.; Song, X.-Q.; Li, F.; Fu, P.-C. Tensile resistance and design model of an external double-layered flange connection. *J. Constr. Steel Res.* **2019**, *161*, 309–372. [[CrossRef](#)]
10. Budynas, R.G.; Nisbett, J.K. *Shigley's Mechanical Engineering Design*; McGrawHill: New York, NY, USA, 2011.
11. Schmid, S.R.; Hamrock, B.J.; Jacobson, B.O. *Fundamentals of Machine Elements*; CRC Press: Boca Raton, FL, USA, 2014.
12. Niemann, G.; Winter, H.; Hohn, B.R.; Stahl, K. *Maschinenelemente 1—Konstruktion und Berechnung von Verbindungen, Lagern, Wellen*; Springer: Berlin/Heidelberg, Germany, 2019.
13. Oman, S.; Nagode, M. Bolted connection of an end-plate cantilever beam: The distribution of operating force. *Stroj. Vestn. J. Mech. Eng.* **2017**, *63*, 617–627. [[CrossRef](#)]
14. Pavlović, M.; Heistermann, C.; Veljković, M.; Pak, D.; Feldmann, M.; Rebelo, C.; daSilva, L.S. Connections in towers for wind converters, part I: Evaluation of down scaled experiments. *J. Constr. Steel Res.* **2015**, *115*, 445–457. [[CrossRef](#)]
15. Zou, T.; Niu, X.; Ji, X.; Li, M.; Tao, L. The Impact of Initial Imperfections on the Fatigue Assessment of Tower Flange Connections in Floating Wind Turbines: A Review. *Front. Mar. Sci.* **2022**, *9*, 1063120. [[CrossRef](#)]
16. Ji, X.; Zou, T.; Bai, X.; Niu, X.; Tao, L. Fatigue Assessment of Flange Connections in Offshore Wind Turbines under the Initial Flatness Divergence. *Front. Energy Res.* **2023**, *11*, 137. [[CrossRef](#)]
17. VDI 2230-1:2015; Systematic Calculation of Highly Stressed Bolted Joints—Joints with One Cylindrical Bolt. VDI-Gesellschaft Produkt-und Prozessgestaltung: Düsseldorf, Germany, 2015.
18. EN 1993-1-9; Eurocode 3: Design of Steel Structures—Part 1-9: Fatigue. European Committee for Standardization (CEN): Brussels, Belgium, 2005.
19. Kloos, K.H.; Thomala, W. *Schraubenverbindungen: Grundlagen, Berechnung, Eigenschaften, Handhabung*; Springer: Berlin, Germany, 2007.
20. Cardoso, R.C.; Nascimento, B.L.; Thompson, F.F.; Griza, S. Study of bolted joint axial stiffness using finite element analyses, experimental tests, and analytical calculations. *Proc. Inst. Mech. Eng. Part C J. Mech. Eng. Sci.* **2020**, *234*, 4671–4681. [[CrossRef](#)]
21. Naruse, T.; Shibutani, Y. Equivalent stiffness evaluations of clamped plates in bolted joints under loading. *J. Solid Mech. Mater. Eng.* **2010**, *2*, 1791–1805. [[CrossRef](#)]
22. Wileman, J.; Choudhury, M.; Green, I. Computation of member stiffness in bolted connections. *ASME J. Mech. Des.* **1991**, *113*, 432–437. [[CrossRef](#)]
23. Haidar, N.; Obeed, S.; Jawad, M. Mathematical representation of bolted-joint stiffness: A new suggested model. *J. Mech. Sci. Technol.* **2011**, *25*, 2827–2834. [[CrossRef](#)]
24. Cao, J.; Zhang, Z. Finite element analysis and mathematical characterization of contact pressure distribution in bolted joints. *J. Mech. Sci. Technol.* **2019**, *33*, 4715–4725. [[CrossRef](#)]
25. Lehnhoff, T.F.; Ko, K.I.; McKay, M.L. Member stiffness and contact pressure distributions of bolted joints. *ASME J. Mech. Des.* **1994**, *116*, 550–557. [[CrossRef](#)]
26. Musto, J.C.; Konkle, N.R. Computation of member stiffness in design of bolted joints. *ASME J. Mech. Des.* **2006**, *128*, 1357–1360. [[CrossRef](#)]
27. Okorn, I.; Nagode, M.; Klemenc, J.; Oman, S. Analysis of Additional Load and Fatigue Life of Preloaded Bolts in a Flange Joint Considering a Bolt Bending Load. *Metals* **2021**, *11*, 449. [[CrossRef](#)]
28. EN 1092-1:2018; Flanges and Their Joints—Circular Flanges for Pipes, Valves, Fittings and Accessories, PN Designated—Part 1: Steel Flanges. European Committee for Standardization (CEN): Brussels, Belgium, 2018.
29. Griza, S.; da Silva, M.E.G.; dos Santos, S.V. The effect of bolt length in the fatigue strength of M24x3 bolt studs. *Eng. Fail. Anal.* **2013**, *34*, 397–406. [[CrossRef](#)]
30. Griza, S.; da Silva, M.E.; dos Santos, S.V.; Strohaecker, T.R. Experimental evaluation of cyclic stresses on axially loaded bolted joints. *Proc. Inst. Mech. Eng. Part C J. Mech. Eng. Sci.* **2016**, *230*, 2611–2622. [[CrossRef](#)]
31. Griza, S.; Bertoni, F.; Zanon, G.; Reguly, A.; Strohaecker, T. Fatigue in engine connecting rod bolt due to forming laps. *Eng. Fail. Anal.* **2009**, *16*, 1542–1548. [[CrossRef](#)]
32. Chang, Y.; Ding, J.; He, Z.; Shehzad, A.; Ding, Y.; Lu, H.; Zhuang, H.; Chen, P.; Zhang, Y.; Zhang, X.; et al. Effect of joint interfacial contact stiffness on structural dynamics of ultra-precision machine tool. *Int. J. Mach. Tools Manuf.* **2020**, *158*, 103609. [[CrossRef](#)]
33. Jiang, K.; Liu, Z.; Yang, C.; Zhang, C.; Tian, Y.; Zhang, T. Effects of the joint surface considering asperity interaction on the bolted joint performance in the bolt tightening process. *Tribol. Int.* **2022**, *167*, 107408. [[CrossRef](#)]
34. Cornwell, R.E. Computation of load factors in bolted connections. *Proc. Inst. Mech. Eng. Part C J. Mech. Eng. Sci.* **2009**, *223*, 795–808. [[CrossRef](#)]
35. Schmidt, H.; Neuper, M. Zum elastostatischen tragverhalten exzentrisch gezogener L-stöße mit vorgespannten schrauben [On the elastostatic behaviour of an eccentrically tensioned L-joint with prestressed bolts]. *Stahlbau* **1997**, *66*, 163–168.
36. Petersen, C. *Stahlbau: Grundlagen der Berechnung und Baulichen Ausbildung von Stahlbauten, [Steel Construction: Fundamentals of Calculation and Structural Design of Steel Structures]*; Springer Vieweg: Wiesbaden, Germany, 2012.
37. Schaumann, P.; Seidel, M. Ermüdungsbeanspruchung geschraubter Ringflanschverbindungen bei Windenergieanlagen, [Fatigue loading of bolted ring flange connections for wind turbines [Ermüdungsbeanspruchung geschraubter Ringflanschverbindungen bei Windenergieanlagen]. *Stahlbau* **2002**, *71*, 204–211. [[CrossRef](#)]
38. Schaumann, P.; Eichstädt, R.; Stang, A. Advanced performance assessment methods for high-strength bolts in ring-flange connections. *Stahlbau* **2018**, *87*, 446–455. [[CrossRef](#)]

39. Cheng, L.; Yang, F.; Seidel, M.; Veljković, M. FE-assisted investigation for mechanical behaviour of connections in offshore wind turbine towers. *Eng. Struct.* **2023**, *285*, 116039. [[CrossRef](#)]
40. Shi, G.; Shi, Y.; Wang, Y.; Bradford, M.A. Numerical simulation of steel pretensioned bolted end-plate connections of different types and details. *Eng. Struct.* **2008**, *30*, 2677–2686. [[CrossRef](#)]
41. Díaz, C.; Victoria, M.; Martí, P.; Querin, O.M. FE model of beam-to-column extended end-plate joints. *J. Constr. Steel Res.* **2011**, *67*, 1578–1590. [[CrossRef](#)]
42. Drosopoulos, G.A.; Stavroulakis, G.E.; Abdalla, K.M. 3D finite element analysis of end-plate steel joints. *Steel Compos. Struct.* **2012**, *12*, 93–115. [[CrossRef](#)]
43. Wang, M.; Shi, Y.; Wang, Y.; Shi, G. Numerical study on seismic behaviours of steel frame end-plate connections. *J. Constr. Steel Res.* **2013**, *90*, 140–152. [[CrossRef](#)]
44. Saberi, V.; Gerami, M.; Kheyroddin, A. Comparison of bolted end plate and T-stub connection sensitivity to component thickness. *J. Constr. Steel Res.* **2014**, *98*, 134–145. [[CrossRef](#)]
45. El-Khoriby, S.; Sakr, A.M.; Khalifa, T.M.; Eladly, M.M. Modeling and behaviour of beam-to-column connections under axial force and cyclic bending. *J. Constr. Steel Res.* **2017**, *129*, 171–184. [[CrossRef](#)]
46. Bartsch, H.; Hoffmeister, B.; Feldmann, M. Fatigue analysis of welds and bolts in end plate connections of I-girders. *Int. J. Fatigue* **2020**, *138*, 105674. [[CrossRef](#)]
47. Bartsch, H.; Feldmann, M. Reassessment of fatigue detail categories of bolts and rods according to EC 3-1-9. *J. Constr. Steel Res.* **2021**, *180*, 106588. [[CrossRef](#)]
48. Wang, Y.Q.; Zong, L.; Shi, Y.J. Bending behavior and design model of bolted flange-plate connection. *J. Constr. Steel Res.* **2013**, *84*, 1–16. [[CrossRef](#)]
49. Couchaux, M.; Hjiiaj, M.; Ryanb, I.; Bureaub, A. Bolted circular flange connections under static bending moment and axial force. *J. Constr. Steel Res.* **2019**, *157*, 314–336. [[CrossRef](#)]
50. Jaszak, P. The elastic serrated gasket of the flange bolted joints. *Int. J. Press. Vessel. Pip.* **2019**, *176*, 103954. [[CrossRef](#)]
51. Adamek, K.; Jaszak, P. Design method of enhancing the tightness of a spiral wound gasket with PTFE filling. *J. Braz. Soc. Mech. Sci. Eng.* **2023**, *45*, 332. [[CrossRef](#)]
52. Slecicka, L.; Len, D. Prying action in bolted circular flange joints: Approach based on component method. *Eng. Struct.* **2021**, *228*, 111528. [[CrossRef](#)]
53. Ajaei, B.B.; Soyoz, S. Effects of preload deficiency on fatigue demands of wind turbine tower bolts. *J. Constr. Steel Res.* **2020**, *166*, 105933. [[CrossRef](#)]
54. Croccolo, D.; De Agostinis, M.; Fini, S.; Mele, M.; Olmi, G. Effect of different underhead shot-peening and lubrication conditions on high-strength screws undergoing multiple tightenings. *Tribol. Int.* **2023**, *188*, 108874. [[CrossRef](#)]
55. Liu, Z.; Jiang, K.; Dong, X.; Zhang, C.; Tian, Y.; Hu, Q. A research method of bearing coefficient in fasteners based on the fractal and Florida theory. *Tribol. Int.* **2020**, *152*, 106544. [[CrossRef](#)]
56. EN 14399-4: 2015-4; High-Strength Structural Bolting Assemblies for Preloading—Part 4: System HV—Hexagon Bolt and Nut Assemblies. European Committee for Standardization (CEN): Brussels, Belgium, 2015.
57. EN 14399-6: 2015-6; High-Strength Structural Bolting Assemblies for Preloading—Part 6: Plain Chamfered Washers. European Committee for Standardization (CEN): Brussels, Belgium, 2015.
58. ISO 4014:2022(E); Fasteners—Hexagon Head Bolts—Product Grades A and B. International Organization for Standardization: Geneva, Switzerland, 2022.
59. ISO 4032:2023; Fasteners—Hexagon Regular Nuts. International Organization for Standardization: Geneva, Switzerland, 2023.
60. Z-14.4-800; Allgemeine Bauaufsichtliche Zulassung/Allgemeine Bauartgenehmigung. IHF Schraubsysteme, DIBt: Berlin, Germany, 2021.
61. Kumar, C.; Mungara, S.R.; Sanjan, J. Design and Analysis of a Compact Hydraulic Bolt Tensioner. *J. Phys. Conf. Ser.* **2022**, *2332*, 012013. [[CrossRef](#)]
62. Zhu, L.; Bouzid, A.H.; Hong, J. Analytical evaluation of elastic interaction in bolted flange joints. *Int. J. Press. Vessel. Pip.* **2018**, *165*, 176–184. [[CrossRef](#)]
63. Grzejda, R.; Warzecha, M.; Urbanowicz, K. Determination of pretension in bolts for structural health monitoring of multi-bolted connection: FEM approach. *Lubricants* **2022**, *10*, 75. [[CrossRef](#)]
64. Grzejda, R.; Parus, A.; Kwiatkowski, K. Experimental studies of an asymmetric multi-bolted connection under monotonic loads. *Materials* **2021**, *14*, 2353. [[CrossRef](#)] [[PubMed](#)]
65. Coria, I.; Abasolo, M.; Aguirrebeitia, J.; Heras, I. Study of bolt load scatter due to tightening sequence. *Int. J. Press. Vessel. Pip.* **2020**, *182*, 104054. [[CrossRef](#)]
66. Wang, Y.; Liu, Z.; Li, Y.; Yang, C. Methodology for optimization of preload in a bolted-flange connection based on Markov theory. *J. Phys. Conf. Ser.* **2022**, *2174*, 12072. [[CrossRef](#)]
67. Braithwaite, J.; Mehmanparast, A. Analysis of tightening sequence effects on preload behaviour of offshore wind turbine M72 bolted connections. *Energies* **2019**, *12*, 4406. [[CrossRef](#)]
68. You, R.; Ren, L.; Song, G. A novel comparative study of European, Chinese and American codes on bolt tightening sequence using smart bolts. *Int. J. Steel Struct.* **2020**, *20*, 910–918. [[CrossRef](#)]

69. Croccolo, D.; De Agostinis, M.; Fini, S.; Khan, M.-J.; Mele, M.; Olmi, G. Optimization of Bolted Joints: A Literature Review. *Metals* **2023**, *13*, 1708. [[CrossRef](#)]
70. Croccolo, D.; De Agostinis, M.; Fini, S.; Mele, M.; Olmi, G.; Scapecchi, C.; Bin Tariq, M.-H. Failure of Threaded Connections: A Literature Review. *Machines* **2023**, *11*, 212. [[CrossRef](#)]
71. Okorn, I.; Nagode, M.; Klemenc, J.; Oman, S. Influence of geometric imperfections of flange joints on the fatigue load of preloaded bolts. *Int. J. Press. Vessel. Pip.* **2024**, *210*, 105237. [[CrossRef](#)]
72. Jakubowski, A.; Schmidt, H. Experimentelle Untersuchungen an vorgespannten Ringflanschstößen mit Imperfektionen [Experimental analysis on preloaded ring flange connections with imperfections]. *Stahlbau* **2003**, *72*, 188–196. [[CrossRef](#)]
73. Schwedler, M.; Dörfeldt, S.; Lüddecke, F.; Seidel, M.; Thiele, M. Einflussfaktoren auf die Vorspannkraft von Schrauben mit Durchmessern bis M72 in Ringflanschverbindungen. *Stahlbau* **2018**, *87*, 149–161. [[CrossRef](#)]
74. Lüddecke, F.; Victor, A.; Schwedler, M. Analyse des Einflusses fertigungsbedingter Imperfektionen auf die Schraubenkraft an großen Ringflanschverbindungen, [Analysis of the influence of flange imperfections due to fabrication tolerances on the bolt force in large ring flange connections]. *Der Prüfmagister* **2019**, *11*, 42–57.
75. Seidel, M. Tolerance requirements for flange connections in wind turbine support structures. *Stahlbau* **2018**, *87*, 880–887. [[CrossRef](#)]
76. Feldmann, M.; Naumes, J.; Pak, D. Zum last-Verformungsverhalten von Schrauben in vorgespannten Ringflanschverbindungen mit überbrückten Klaffungen im Hinblick auf die Ermüdungsvorhersage, [On the load-deformation behaviour of bolts in preloaded ring flange connections with gaps with regard to fatigue prediction]. *Stahlbau* **2011**, *80*, 21–29.
77. Tran, T.-T.; Park, H.; Lee, D. Structural Behavior of L-Type Flange Joint with Various Flange Flatness Conditions. *Energies* **2023**, *16*, 5703. [[CrossRef](#)]
78. Seidel, M.; Stang, A.; Wegener, F.; Schierl, C.; Schaumann, P. Full-scale validation of FE models for geometrically imperfect flange connections. *J. Constr. Steel Res.* **2021**, *187*, 106955. [[CrossRef](#)]
79. Weijtjens, W.; Stang, A.; Devriendt, C.; Schaumann, P. Bolted ring flanges in offshore-wind support structures-in-situ validation of load-transfer behaviour. *J. Constr. Steel Res.* **2021**, *176*, 106361. [[CrossRef](#)]
80. Abdelrahman, M.-S.; Khalifa, W.; Abdu, M.-T. Failure analysis of fatigue failed M20 class 8.8 galvanized steel bolt. *Eng. Fail. Anal.* **2023**, *150*, 107304. [[CrossRef](#)]
81. Jiao, J.; Liu, Z.; Guo, Q.; Liu, Y.; Lei, H. Constant-amplitude fatigue behavior of M24 high-strength bolt of end-plate flange connection. *Structures* **2021**, *34*, 2041–2053. [[CrossRef](#)]
82. Welch, M. Fatigue Analysis of Preloaded Bolted Joints. *FME Trans.* **2022**, *50*, 607–614. [[CrossRef](#)]
83. Glienke, R.; Schwarz, M.; Marten, F.; Eichstädt, R.; Schwerdt, D.; Meyer, M.; Dörre, M. Zur ermüdungsfestigkeit großer Schrauben im Stahlbau unter Berücksichtigung von Herstell- und Randschichteinflüssen—Teil 1: Bisheriger Kenntnisstand [On fatigue strength of large-size bolt-assemblies in steel constructions under consideration of manufacturing and surface condition related impacts—Part 1: State of knowledge]. *Stahlbau* **2022**, *91*, 10–19.
84. Glienke, R.; Schwarz, M.; Marten, F.; Eichstädt, R.; Schwerdt, D.; Meyer, M.; Dörre, M. Zur ermüdungsfestigkeit großer Schrauben im Stahlbau unter Berücksichtigung von Herstell- und Randschichteinflüssen—Teil 2: Versuchsergebnisse und Bewertung [On fatigue strength of large-size bolt-assemblies in steel constructions under consideration of manufacturing and surface condition related impacts—Part 2: Evaluation of fatigue tests]. *Stahlbau* **2022**, *91*, 20–38.
85. EN 13001-3-1:2018; Cranes—General Design—Part 3-1: Limit States and Proof Competence of Steel Structure. International Organization for Standardization: Geneva, Switzerland, 2018.
86. Maljaars, J.; Euler, M. Fatigue S-N curves of bolts and bolted connections for application in civil engineering structures. *Int. J. Fatigue* **2021**, *151*, 106355. [[CrossRef](#)]
87. Govindu, N.; Jayanand Kumar, T.; Venkadesh, S. Design and optimization of screwed fasteners to reduce stress concentration factor. *J. Appl. Mech. Eng.* **2015**, *4*, 1000171.
88. Brutti, C. Load and stress distribution in screw threads with modified washers. *J. Multidiscip. Eng. Sci. Technol.* **2017**, *4*, 6523–6533.
89. Lee, C.H.; Kim, B.J.; Han, S.Y. Mechanism for reducing stress concentrations in bolt-nut connectors. *Int. J. Precis. Eng. Manuf.* **2014**, *15*, 1337–1343. [[CrossRef](#)]
90. Noda, N.A.; Wang, B.; Oda, K.; Sano, Y.; Liu, X.; Inui, Y.; Yakushiji, T. Effects of root radius and pitch difference on fatigue strength and anti-loosening performance for high strength bolt–nut connections. *Adv. Struct. Eng.* **2021**, *24*, 1941–1954. [[CrossRef](#)]
91. Coria, I.; Abasolo, M.; Gutiérrez, A.; Aguirrebeitia, J. Achieving uniform thread load distribution in bolted joints using different pitch values. *Mech. Ind.* **2020**, *21*, 616. [[CrossRef](#)]
92. Matsunari, T.; Oda, K.; Tsutsumi, N.; Yakushiji, T.; Noda, N.A.; Sano, Y. Experimental study on the effect of shape of bolt and nut on fatigue strength for bolted joint. *IOP Conf. Ser. Mater. Sci. Eng.* **2018**, *372*, 012016. [[CrossRef](#)]
93. Pedersen, N.L. Optimization of bolt thread stress concentrations. *Arch. Appl. Mech.* **2013**, *83*, 1–14. [[CrossRef](#)]
94. Pedersen, N.L. Optimization of bolt stress. In Proceedings of the 10th World Congress on Structural and Multidisciplinary Optimization, Orlando, FL, USA, 19–24 May 2013; pp. 142–148.

95. Reggiani, B.; Olmi, G. Experimental investigation on the effect of shot peening and deep rolling on the fatigue response of high strength fasteners. *Metals* **2019**, *9*, 1093. [[CrossRef](#)]
96. Wang, X.; Xiong, X.; Huang, K.; Ying, S.; Tang, M.; Qu, X.; Ji, W.; Qian, C.; Cai, Z. Effects of Deep Rolling on the Microstructure Modification and Fatigue Life of 35Cr2Ni4MoA Bolt Threads. *Metals* **2022**, *12*, 1224. [[CrossRef](#)]

**Disclaimer/Publisher's Note:** The statements, opinions and data contained in all publications are solely those of the individual author(s) and contributor(s) and not of MDPI and/or the editor(s). MDPI and/or the editor(s) disclaim responsibility for any injury to people or property resulting from any ideas, methods, instructions or products referred to in the content.